

Calculating Fermion Yukawa Couplings in M-Theory, and Early Universe Cosmology with Axions

by

Eric Gonzalez

A dissertation submitted in partial fulfillment
of the requirements for the degree of
Doctor of Philosophy
(Physics)
in The University of Michigan
2021

Doctoral Committee:

Professor Emeritus Gordon Kane, Chair
Professor Lydia Bieri
Professor Dragan Huterer
Assistant Professor Bjoern Penning
Professor Aaron Pierce

Eric Gonzalez

ericgz@umich.edu

ORCID iD: [0000-0002-5028-7607](https://orcid.org/0000-0002-5028-7607)

For my partner Mariah, and my family.

ACKNOWLEDGEMENTS

Special thanks to my advisor Professor Gordon Kane, for the opportunity to work with him on deep and fundamental problems, for his unwavering support, and for his wisdom and guidance which helped make this possible. Thanks to all the members of my dissertation committee, Professors Aaron Pierce, Dragan Huterer, Lydia Bieri, and Bjoern Penning for their help and guidance through the process of writing my dissertation and defending my thesis. Special thanks to Raymond Co and Keisuke Harigaya for their time and efforts in our collaborations, their excellent mentorship has made me a better scientist. Thanks to all the members of the Leinweber Center for Theoretical Physics, who welcomed me from the first day and have given me advice throughout my candidacy. Thanks to my peers, Shruti Paranjape, Joshua Foster, Noah Steinberg, Matthew Day, Garrett Merz, Rachel Owen, and Khoa Dang Nguyen for their knowledge, advice, friendship, and support.

TABLE OF CONTENTS

DEDICATION	ii
ACKNOWLEDGEMENTS	iii
LIST OF FIGURES	vi
LIST OF TABLES	vii
ABSTRACT	viii
CHAPTER	
I. Introduction	1
1.1 The Standard Model	2
1.1.1 The QCD Sector	3
1.1.2 The Electroweak Sector	3
1.1.3 The Yukawa Sector	5
1.2 Supersymmetry	6
1.3 Cosmology and Particle Physics	9
1.4 Axions and the Misalignment Mechanism	12
II. Yukawa Couplings in the String Landscape	16
2.1 M-theory and Manifolds of G_2 Holonomy	16
2.2 E_8 Unification	19
2.2.1 Fermion Representations	23
2.3 Yukawa Couplings from Three-Cycle Volumes	24
2.4 Quark Terms	27
2.4.1 General Quark Terms	27
2.4.2 Diagonal Terms and Setting $a = 0$	28
2.4.3 Quark Mass Matrices	29
2.4.4 Six Higgs VEVs	30
2.4.5 Higgs VEVs	32

2.5	Yukawa matrix for gauge group $SU(3) \times SU(2) \times U(1)^Y \times U(1)^b \times U(1)^c \times U(1)^d$	32
2.6	Computational Setup	33
2.7	Numerical Evaluation	34
III. Axions Dynamically Driven to the Hilltop		37
3.1	Introduction	37
3.2	Dynamical Axion Misalignment Production at the Hilltop	40
3.2.1	Axion Mass During Inflation	42
3.2.2	Shifted Axion Potential	45
3.3	Cosmological Evolution	46
3.3.1	Minimal Models	46
3.3.2	Extended Models	51
IV. Axions Dynamically Driven to the Origin		56
4.1	Misalignment Mechanism	59
4.2	Early Relaxation during Inflation	60
V. Conclusion		67
5.1	Yukawa Couplings	67
5.2	Dynamical Axion Misalignment Production	68
BIBLIOGRAPHY		72

LIST OF FIGURES

Figure

2.1	An A_3 type singularity being fully resolved will have a configuration of three Riemann spheres $\mathbb{P}^1(\mathbb{C})$ which intersect according to A_3 Dynkin diagram.	18
2.2	Dynkin diagram and associated groups.	19
2.3	Breaking of E_8 by resolving singularity	21
2.4	A set of sample solutions found numerically. The three symbols indicate three different solutions, and the line indicates the measured value for each Yukawa coupling.	35
3.1	Parameter space for the inflationary Hubble scale H_I and reheat temperature T_R given $f_a = 3 \times 10^9$ GeV, $m_{\tilde{g}} = m_{\text{SUSY}} = \text{TeV}$, $B\mu = m_{\text{SUSY}}^2 / \tan \beta$, $\tan \beta = 50$, $N_e = 60$, and $\phi_i = M$. The left (right) panel is for the cutoff scale $M = M_{\text{GUT}}$ (M_{Pl}) respectively.	47
3.2	Parameter space for the inflationary Hubble scale H_I and the fiducial confinement scale Λ_{fid} defined in Eq. (3.8) given $f_a = 3 \times 10^9$ GeV, $m_{\tilde{g}} = m_{\text{SUSY}} = \text{TeV}$, and $\phi_i = M$. The left (right) panel is for the cutoff scale $M = M_{\text{GUT}}$ (M_{Pl}) respectively.	54
4.1	Parameter space for the inflationary Hubble scale H_I and the fiducial confinement scale Λ_{fid} defined in Eq. (4.10) given $m_{\tilde{g}} = m_{\text{SUSY}} = \text{TeV}$, and $\phi_i = M$. The left (right) panel is for the cutoff scale $M = M_{\text{GUT}}$ (M_{Pl}) respectively.	66

LIST OF TABLES

Table

1.1	The Standard Model particle content, not including quark and lepton family generations along with their G_{SM} and Spin representations. . .	2
1.2	The MSSM superpartners to the SM fields in Table. 1.2, their G_{SM} representations and spins. We also include the new pair of Higgs doublets Φ_u and Φ_d which replace the Φ in Eq. 1.1	7
2.1	Positive roots of E_n and the associated one-forms (sometimes called “area” in literature) controlling the sizes of 2-cycles on the ALE fiber.	20
2.2	Constraints required to preserve \mathcal{G}_{SM} and break the other E_8 subgroup symmetries.	23
2.3	Relevant particles from three families of E_6	24
2.4	GUT scale Yukawa couplings from [131].	34

ABSTRACT

In this dissertation, we discuss work done to explore the parameter space of geometric engineering with M-theory on manifolds of G_2 holonomy. The local geometry of the G_2 manifold is related to the Yukawa coupling constants observed in the standard model via moduli vacuum expectation values. Using stochastic gradient descent, we find a point in an expansive parameter space of moduli consistent with measured values of Yukawa couplings. Additionally, work was done to explore the cosmological viability of dark matter axions with large and small decay constants f_a . By permitting a Hubble induced mass term to modify the Higgs scalar potential in the early universe, we show that early universe dark matter axion dynamics can reproduce the observed dark matter abundance $\Omega_{\text{DM}}h^2 = 0.12$ with a decay constant smaller or larger than the typical $f_a \simeq 10^{12}$ GeV required by the usual misalignment mechanism.

CHAPTER I

Introduction

This dissertation covers two important phenomenological aspects of String Theory, primarily within the framework of M-Theory compactified on a manifold of G_2 holonomy. In the first part we discuss work done to calculate the Yukawa couplings of Standard Model Fermions (up, down, and electron families) as well as the Yukawa and Majorana couplings of the neutrinos within the context of M-Theory with a compactification manifold of G_2 holonomy. In the second part we discuss a theoretical method for setting initial misalignment angle for an axion or axion like particle (ALP) to the minimum or maximum of its potential.

The importance of studying M-Theory lies in the fact that it is a UV complete theory which may resolve many long standing mysteries of modern physics. In order to better understand how M-Theory solves these problems we will discuss the status of modern physics and how the current body of work on M-Theory resolves the issues in the remainder of the Chapter I. In Chapter II we will detail our work done to calculate Yukawa coupling terms in M-Theory. In Chapter III and Chapter IV we will discuss the Dynamical Axion Misalignment Production (DAMP) mechanism which gives us a method for setting the misalignment angle for an ALP to 0 or π , as is preferred or required in various phenomenological models. Finally, in Chapter V we discuss the implications of the work done for both M-Theory and future studies.

1.1 The Standard Model

The Standard Model of Particle Physics is a triumph of modern physics and has accurately described most microscopic phenomena up to the TeV scale, and was completed with the discovery of the Higgs Boson in 2012 [1]. There are various principles and experimental results which have led us to believe that the SM is not the full picture. The goal of this section is to review the quantum field theory that is the Standard Model (SM) and to mention shortcomings of the SM along the way. We begin with a discussion of the symmetries exhibited by the standard model, then explicitly discuss the terms in the SM Lagrangian.

Field	$SU(3)_{\text{QCD}}$	$SU(2)_L$	$U(1)_Y$	Spin
G_μ^a	8	1	0	1
W_μ^a	1	3	0	1
B_μ	1	1	0	1
$Q^i = \begin{pmatrix} u \\ d \end{pmatrix}_L, \begin{pmatrix} c \\ s \end{pmatrix}_L, \begin{pmatrix} t \\ b \end{pmatrix}_L$	3	2	1/6	1/2
$u_R^i = (u_R, c_R, t_R)$	$\bar{\mathbf{3}}$	1	-2/3	1/2
$d_R^i = (d_R, s_R, b_R)$	$\bar{\mathbf{3}}$	1	1/3	1/2
$L^i = \begin{pmatrix} \nu_e \\ e \end{pmatrix}_L, \begin{pmatrix} \nu_\mu \\ \mu \end{pmatrix}_L, \begin{pmatrix} \nu_\tau \\ \tau \end{pmatrix}_L$	1	2	-1/2	1/2
$e_R^i = (e_R, \mu_R, \tau_R)$	1	1	1	1/2
$\Phi = \begin{pmatrix} \phi^+ \\ \phi^0 \end{pmatrix}$	1	2	1/2	0

Table 1.1: The Standard Model particle content, not including quark and lepton family generations along with their G_{SM} and Spin representations.

The symmetry group of the Standard Model (SM) consists of the gauge symmetry group $\mathcal{G}_{\text{SM}} = U(1)_Y \times SU(2)_L \times SU(3)_{\text{QCD}}$ and the Poincaré group $SO^+(3,1)$. A requirement for a valid SM interaction is that it should be invariant under symmetry group transformations, i.e. individual terms should be composed of fields whose tensor

product is a singlet under all group transformations. We will divide the standard model into three sectors to highlight particular problems of interest within those sectors.

1.1.1 The QCD Sector

The QCD sector contains the kinetic terms for the fundamental particles charged under $SU(3)_{\text{QCD}}$, which reads

$$\mathcal{L}_{\text{QCD}} = \sum_{\psi, \bar{\psi}} i\bar{\psi} \not{D}\psi - \frac{1}{4} G_{\mu\nu}^a G_a^{\mu\nu}. \quad (1.1)$$

Where we sum over fields $\psi(\bar{\psi})$ in the (anti-)fundamental representation, $\mathbf{3}(\bar{\mathbf{3}})$. A topological term which violates CP but respects $SU(3)_c$ is allowed, written as

$$\mathcal{L}_{\text{QCD}'} \supset -\frac{\bar{\theta} g_3^2}{32\pi^2} \tilde{G}_{\mu\nu}^a G_a^{\mu\nu}, \quad (1.2)$$

with QCD vacuum angle $\bar{\theta}$. This vacuum angle $\bar{\theta} = \theta - \arg(\det M)$ gets a contribution θ from the topology of vacuum gauge field configurations and $\arg(\det M)$ from the chiral anomaly [139, 90]. In principle this angle can be anywhere on the interval $[0, 2\pi)$, and measurements of the neutron electric dipole moment place a limit on the value at $|\bar{\theta}| < 3 \times 10^{-10}$ [126]. This gives rise to a problem known as the **Strong CP Problem** [57, 139].

1.1.2 The Electroweak Sector

The Electroweak sector contains the kinetic terms for fields charged under $SU(2)_L \times U(1)_Y$, which reduces to $U(1)_{\text{EM}}$ when the $SU(2)_L \times U(1)_Y$ symmetry is broken by the Higgs mechanism. Above the Electroweak Symmetry Breaking (EWSB) scale

$v_{\text{EW}} \sim 175$ GeV the electroweak Lagrangian reads

$$\mathcal{L}_{\text{EW}} = \sum_{\psi, \bar{\psi}} i\bar{\psi}\not{D}\psi - \frac{1}{4}W_{\mu\nu}^a W_a^{\mu\nu} - \frac{1}{4}B_{\mu\nu}B^{\mu\nu} + |(D_\mu\Phi)|^2 + \mu^2\Phi^\dagger\Phi - \lambda(\Phi^\dagger\Phi)^2, \quad (1.3)$$

where we have summed over all fields ψ charged under $SU(2)_L$ and/or $U(1)_Y$. The Higgs scalar potential $V(\Phi) = -\mu^2|\Phi|^2 + \lambda|\Phi|^4$ induces EWSB when the Higgs field acquires a vacuum expectation value (vev) $\langle 0|\Phi|0\rangle = \frac{v}{\sqrt{2}}$ with $v = \frac{\mu}{\sqrt{\lambda}}$. Once the Higgs vev is non-vanishing, we rewrite the electroweak Lagrangian in terms of mass eigenstates of the now massive gauge bosons and the massless photon from the residual $U(1)_{\text{EM}}$,

$$\begin{aligned} \mathcal{L}_{\text{EW}'} = & \sum_{\psi, \bar{\psi}} i\bar{\psi}\not{D}\psi - \frac{1}{4}F_{\mu\nu}F^{\mu\nu} - \frac{1}{4}Z_{\mu\nu}Z^{\mu\nu} + \frac{1}{2}m_Z^2 Z^\mu Z_\mu \\ & - \frac{1}{4}W_{\mu\nu}^\pm W^{\pm\mu\nu} + \frac{1}{2}m_W^2 W_\mu^\pm W^{\pm\mu} + |(\partial_\mu h)|^2 - V(h). \end{aligned} \quad (1.4)$$

The Higgs mechanism is a boon to the standard model as it explains how the electroweak symmetry is broken, yet the measured Higgs mass is $m_H = 125.10 \pm 0.14$ GeV [143] which is incredibly small compared to the SM quantum corrections it receives from coupling to other fields. At the one loop level, the corrections from SM fermions to the Higgs mass are of order

$$\Delta\mu^2 = \sum_f -\frac{3|Y_f|^2}{8\pi}\Lambda^2 + \dots, \quad (1.5)$$

where Y_f are the SM Yukawa couplings for each massive fermion f and Λ is an ultraviolet (UV) cutoff scale, which can be as large as $M_{\text{pl}} \simeq 10^{19}$ GeV. In the extreme case of $\Lambda = M_{\text{pl}}$, the mass squared corrections are more than 30 orders of magnitude larger than the observed mass, presenting a fine-tuning problem called the **Hierarchy Problem**. One solution, arguable the most simple, is to extend the SM to include **supersymmetry** which will be discussed in Sec. 1.2.

1.1.3 The Yukawa Sector

When the electroweak symmetry is broken by the Higgs mechanism, the vev of the Higgs also gives mass to the quarks and leptons in the SM. The Yukawa sector Lagrangian in the SM is

$$\mathcal{L}_{\text{yukawa}} = \mathbf{Y}_u^{ij} \bar{Q}^i \tilde{\Phi} u_R^j + \mathbf{Y}_d^{ij} \bar{Q}^i \Phi d_R^j + \mathbf{Y}_e^{ij} \bar{L}^i \Phi e_R^j. \quad (1.6)$$

We note that the couplings \mathbf{Y}_u , \mathbf{Y}_d , and \mathbf{Y}_e are 3×3 matrices of couplings, and u_R , d_R , e_R , Q , and L are corresponding vectors in the fermion families space with equivalent quantum numbers. The SM families consist of the up-type quarks, \mathbf{t} , \mathbf{c} , and \mathbf{u} , the down type quarks, \mathbf{b} , \mathbf{s} , and \mathbf{d} , and the electron-type leptons τ , μ , and \mathbf{e} . The observation of three generations in each quark and lepton family, without an understanding of their origin, is known as the **Family Problem**. A common solution to the family problem is to add a global or gauge $SU(3)$ symmetry and place each family in a triplet representation of the symmetry, but without a natural explanation for the hierarchical symmetry breaking (e.g. $m_t > m_c > m_u$) the problem is not actually resolved. In this dissertation, we will present an exciting and novel solution to the **Family Problem** and simultaneously present a first principles calculation of the Yukawa couplings themselves. This solution involves using string moduli to systematically break an E_8 symmetry down to the standard model gauge group, and along the way we find we can calculate the Yukawa couplings directly and give reason to the existence of three distinct families of particles.

Now that we have an idea of some problems we wish to solve, namely the **Strong CP problem**, the **Heirarchy problem**, and the **Family problem**, we will continue the with a brief overview of Supersymmetry.

1.2 Supersymmetry

The importance of studying supersymmetry cannot be overstated. The string theories which are compatible with phenomenological observations of our universe are all superstring theories, and their 4D effective theories include $\mathcal{N} = 1$ supersymmetry.

Supersymmetry (SUSY) is a symmetry between half integer spin fields, fermions, and integer spin fields, bosons. A supersymmetry transformation will transform a fermion into a boson and vice-versa. The generators of the supersymmetry algebra are anticommuting spinors [112],

$$\{Q_\alpha, Q_\alpha^\dagger\} = -2\sigma_{\alpha\dot{\alpha}}^\mu P_\mu. \quad (1.7)$$

Fields which are related to one another by a SUSY transformation form a representation called a *supermultiplet*. For supersymmetric extensions of the standard model, two types are important:

- *Chiral Supermultiplets* contains spin 0 bosons paired to spin 1/2 fermions.
- *Vector Supermultiplets* contain spin 1/2 fermions paired to spin 1 bosons.

The bosonic fields and fermionic fields which reside in a representation of the supersymmetry are said to be superpartners. A symmetry between fermions and bosons could be a boon to the standard model, as it is a straightforward way to solve the Hierarchy problem introduced in Sec. 1.1.2, since bosons and fermions contribute to mass corrections with opposite signs. If there exists an superpartner for each field in the SM that couples to the Higgs field, there would be a systematic cancellation of the large mass corrections from each field. Physicists have developed a minimal extension to the standard model which includes SUSY; it is called the **Minimal Supersymmetric Standard Model** (MSSM).

The SUSY generators Q_α and Q_α^\dagger commute with gauge transformations, implying

Field	$SU(3)_{\text{QCD}}$	$SU(2)_L$	$U(1)_Y$	Spin
\tilde{g}_μ^a	8	1	0	1/2
\tilde{W}_μ^a	1	3	0	1/2
\tilde{B}_μ	1	1	0	1/2
$\tilde{Q}^i = \begin{pmatrix} \tilde{u} \\ \tilde{d} \end{pmatrix}_L, \begin{pmatrix} \tilde{c} \\ \tilde{s} \end{pmatrix}_L, \begin{pmatrix} \tilde{t} \\ \tilde{b} \end{pmatrix}_L$	3	2	1/6	0
$\tilde{u}_R^i = (\tilde{u}_R, \tilde{c}_R, \tilde{t}_R)$	$\bar{\mathbf{3}}$	1	-2/3	0
$\tilde{d}_R^i = (\tilde{d}_R, \tilde{s}_R, \tilde{b}_R)$	$\bar{\mathbf{3}}$	1	1/3	0
$\tilde{L}^i = \begin{pmatrix} \tilde{\nu}_e \\ \tilde{e} \end{pmatrix}_L, \begin{pmatrix} \tilde{\nu}_\mu \\ \tilde{\mu} \end{pmatrix}_L, \begin{pmatrix} \tilde{\nu}_\tau \\ \tilde{\tau} \end{pmatrix}_L$	1	2	-1/2	0
$\tilde{e}_R^i = (\tilde{e}_R, \tilde{\mu}_R, \tilde{\tau}_R)$	1	1	-1/2	0
$\tilde{\Phi}_u = \begin{pmatrix} \tilde{\phi}_u^+ \\ \tilde{\phi}_u^0 \end{pmatrix}$	1	2	1/2	1/2
$\tilde{\Phi}_d = \begin{pmatrix} \tilde{\phi}_d^0 \\ \tilde{\phi}_d^- \end{pmatrix}$	1	2	-1/2	1/2
$\Phi_u = \begin{pmatrix} \phi_u^+ \\ \phi_u^0 \end{pmatrix}$	1	2	1/2	0
$\Phi_d = \begin{pmatrix} \phi_d^0 \\ \phi_d^- \end{pmatrix}$	1	2	-1/2	0

Table 1.2: The MSSM superpartners to the SM fields in Table. 1.2, their G_{SM} representations and spins. We also include the new pair of Higgs doublets Φ_u and Φ_d which replace the Φ in Eq. 1.1

that fields in the same supermultiplet should have the same representation under \mathcal{G}_{SM} . In Table we show the MSSM superpartner for each SM field. We note that the MSSM requires a pair of Higgs doublets instead of one Higgs doublet¹.

Since supersymmetry is a global symmetry, one can show that the operators which

¹The chiral anomaly vanishes if the trace over all charges in a given gauge group is zero; this works out for the standard model but the MSSM extension requires an additional Higgs doublet to cancel the anomaly. Additionally, the superfield formulation restricts the superpotential to be holomorphic in the grassmanian coordinates θ , and no such $i\sigma_2\Phi$ term is allowed.

generate SUSY transformations commute with space-time translations,

$$[Q, P^\mu] = 0 \quad [Q^\dagger, P^\mu] = 0 \quad (1.8)$$

Moreover, the SUSY generators commute with $-P^2$, implying that superpartners share mass eigenvalues. Since superpartners have not been observed, this implies that SUSY must be broken at some scale. We can parametrize our ignorance of SUSY breaking by writing the soft SUSY breaking Lagrangian which explicitly breaks supersymmetry

$$\begin{aligned} \mathcal{L}_{\text{soft}}^{\text{MSSM}} = & -\frac{1}{2} \left(M_1 \tilde{B} \tilde{B} + M_2 \tilde{W}^a \tilde{W}_a + M_3 \tilde{G}^a \tilde{G}_a + c.c. \right) \\ & - \left(A_u^{ij} \tilde{u}_R^i \Phi_u \tilde{Q}_L^j + A_d^{ij} \tilde{d}_R^i \Phi_d \tilde{Q}_L^j + A_e^{ij} \tilde{e}_R^i \Phi_d \tilde{L}_L^j + c.c. \right) \\ & - \left(\tilde{Q}_L^\dagger m_{\tilde{Q}}^2 \tilde{Q}_L + \tilde{L}_L^\dagger m_{\tilde{L}}^2 \tilde{L}_L + \tilde{u}_R^\dagger m_{\tilde{u}}^2 \tilde{u}_R + \tilde{d}_R^\dagger m_{\tilde{d}}^2 \tilde{d}_R + \tilde{e}_R^\dagger m_{\tilde{e}}^2 \tilde{e}_R \right) \\ & - m_{\Phi_u}^2 \Phi_u^* \Phi_u - m_{\Phi_d}^2 \Phi_d^* \Phi_d - (b \Phi_u \Phi_d + c.c.) \end{aligned} \quad (1.9)$$

While the SUSY preserving part of the MSSM Lagrangian introduces no new parameters, in Eq. 1.9 we have introduced many new parameters to account for SUSY breaking. Experimental limits have been placed on these parameters, but thus far no indications of supersymmetric processes have been observed by modern experiments [38]. Some would argue that introducing 105 new parameters in the form of $\mathcal{L}_{\text{soft}}^{\text{MSSM}}$ is not a great solution to the fine-tuning Hierarchy problem, but this is not the only purpose of supersymmetry. Indeed, one of the largest problems with the field theory description of fundamental physics is failure to include gravitation due to non-renormalizability [140]. Few solutions for this problem exist, but one of the most promising is to work within the framework of string theory. In the next section, we will discuss using strings to formulate a UV completion of the standard model.

1.3 Cosmology and Particle Physics

Apart from observations made in high energy collisions, the study of high energy physics is also informed by cosmological observations. The reason for this is that we can extrapolate the evolution of the universe back in time to a singularity event called the Big Bang and moments after the big bang the universe was extremely hot. This implies that physical states with characteristic energies of up to M_{Pl} were accessible, therefore the evolution of the universe after the Big Bang was governed by fundamental interactions. By considering various cosmological observations, we can set up the framework for modern cosmology and introduce puzzles which can be solved with extensions/UV completions of the SM.

The first observation we consider is measurements of the redshift of extra-galactic objects, first done in [155] with dozens more catalogues done in recent years. These catalogues show that there is a systematic tendency for the light emitted by objects in any direction of the sky to be redshifted, implying that all objects are moving away from us. The isotropic redshift along with Poincaré invariance together imply that each point in space is moving away from all other points in space i.e. we live in an expanding universe. In an expanding universe, the cosmological redshift z is defined as

$$z \equiv \frac{\lambda_{\text{obs}}}{\lambda_{\text{emit}}} - 1 \quad (1.10)$$

where λ_{obs} is the wavelength of the observed light and λ_{emit} is the wavelength of the light when it was emitted.

Another critical cosmological observation is the measurement of the *Cosmic Microwave Background* (CMB). The CMB is a map of the light from the early universe, which can be traced back to the surface of last scattering. The surface of last scattering is a space-time event related to recombination, the cosmological era when the universe was cool enough (due to expansion) to allow charge-neutral bound states to

form. Recombination marks the time at which the universe became transparent to radiation, around $z = 1100$. The CMB is therefore a measurement of the distribution of radiation in the early universe. The CMB has a thermal black body spectrum corresponding to a temperature of 2.72548 ± 0.00057 K, hence anisotropies in the CMB are smaller than one part in 10^4 [67]. If we look at two points in the sky with large angular separation, measurements of the CMB imply that these points were in thermal equilibrium, yet they are apparently causally disconnected, implying a high degree of fine tuning in the initial conditions of the universe. This fine tuning problem is called the **Horizon Problem**. The most favored solution to the Horizon Problem is to invoke Inflation - a period of rapid expansion in the early universe. Inflation seems to imply a time-dependent scale factor for the metric of space-time, as we will see momentarily in Eq. 1.11.

By considering the conclusions of the observations just introduced, we can write a space-time metric which takes into account both the isotropy/homogeneity of the universe and the expansion of the universe. Much of modern cosmology is built upon the Friedmann-Lemaître-Robertson-Walker (FLRW) metric,

$$ds^2 = c^2 dt^2 - a(t)d\Sigma^2 \tag{1.11}$$

where $a(t)$ is the *scale factor* and $d\Sigma$ is the metric over three spatial dimensions with uniform curvature (elliptical, Euclidian, or hyperbolic). In particular,

$$d\Sigma^2 = \frac{dr^2}{1 - kr^2} + dr^2 d\Omega^2, \tag{1.12}$$

where $d\Omega^2 = d\theta^2 + \sin^2(\theta) d\phi^2$. In Eq. 1.12, k parametrizes the curvature with $k < 0$ giving hyperbolic space (negative curvature), $k = 0$ Euclidian space, and $k > 0$ elliptical space (positive curvature). The metric in Eq. 1.11 is a solution to Einstein's field equations under the assumptions of an isotropic, homogeneous, and expanding

universe. To understand the dynamics that come from a time dependent scale factor, we use this metric in the Einstein field equations,

$$\mathcal{R}_{\mu\nu} + \mathcal{R}g_{\mu\nu} \equiv G_{\mu\nu} = 8\pi G_{\text{N}}T_{\mu\nu} + \Lambda g_{\mu\nu}, \quad (1.13)$$

where $G_{\mu\nu}$ is the Einstein tensor, $T_{\mu\nu}$ is the stress-energy tensor, and Λ is the cosmological constant. If we extend our assumption of an isotropic and homogeneous universe to the stress-energy tensor, we find that the stress-energy tensor can be characterized by a perfect fluid with time-dependent energy density $\rho(t)$ and pressure $p(t)$, giving $T_{\mu\nu} = \text{diag}(\rho, -p, -p, -p)$ [107]. We can relate the energy density to the pressure via the equation of state $\rho = wp$, and using conservation of stress-energy, one can show $\rho \propto a^{-3(1+w)}$ [107]. For radiation, $w = 1/3$ and for matter $w = 0$, implying $\rho_{\text{R}} \propto a^{-4}$ and $\rho_{\text{M}} \propto a^{-3}$. With expressions for the metric and the stress-energy tensor, solve the Einstein field equations and write the *Friedmann Equations*. The 0-0 component of the Einstein tensor gives

$$\frac{\dot{a}^2}{a^2} + \frac{k}{a^2} = \frac{8\pi G_{\text{N}}}{3}\rho, \quad (1.14)$$

and the i - i components give

$$2\frac{\ddot{a}}{a} + \frac{\dot{a}^2}{a^2} + \frac{k}{a^2} = -8\pi G_{\text{N}}p. \quad (1.15)$$

It is standard to define the *Hubble Parameter*,

$$H = \frac{\dot{a}}{a}, \quad (1.16)$$

and rewrite Eq. 1.14 as

$$\frac{k}{H^2 a^2} = \frac{8\pi G_{\text{N}}}{3H^2}\rho - 1 = \Omega - 1 \quad \text{https://www.overleaf.com/project/60b50b9b7085e982abd93b7e} \quad (1.17)$$

where we have defined Ω as the ratio of density ρ to critical density $\rho_C = \frac{3H^2}{8\pi G_N}$. Measurements indicate that $\Omega = 1$ to 0.2% precision, implying $k = 0$, i.e. the universe is approximately flat². The CMB has also allowed us to measure the proportion of the total energy density that is in matter, radiation, and vacuum energy. Recent results from the Planck collaboration indicate that dark energy dominates the energy density with $\Omega_\Lambda = 0.626 \pm 0.020$, while matter contributes $\Omega_m = 0.314 \pm 0.020$ [16]. Interestingly, many experiments have shown evidence of **Dark Matter**, a substance which has the gravitational properties of matter, but does not interact via the electromagnetic force³. According to the Planck collaboration, the matter energy density ratio is split into baryons and cold dark matter $\Omega_m = \Omega_b + \Omega_c$, with roughly 15.5% of the matter attributed to baryons, and the other 84.5% to dark matter. Apart from the CMB, evidence in favor of particle dark matter comes from sources such as galaxy cluster mass measurements [156], galaxy rotation curves [132], velocity dispersion measurements [65], galaxy cluster x-ray emission measurements [18], gravitational lensing measurements [115, 130], the Bullet cluster [48], and much more.

In this section, we came to the conclusion that to a first approximation, the universe is isotropic, homogeneous, flat, and expanding. These conclusions are primarily driven by measurements of the CMB anisotropy. We also introduced the concept of dark matter, whose physical nature is one of the largest open problems in physics today.

1.4 Axions and the Misalignment Mechanism

In the Standard Model, a dimensionless charge conjugation and parity (CP) violating parameter θ is constrained to be less than $\mathcal{O}(10^{-10})$ by the experimental

²This is another cosmological fine-tuning problem called the **Flatness Problem**, since a flat universe is metastable and even slight departures from $\Omega = 1$ or $\rho_C \neq \rho$ are amplified by the expansion of the universe. A precision of one part in 10^2 means that the universe was flat to within one part in 10^{60} during the Planck Era [16, 86, 77]

³Although we have not detected interactions with dark matter via the electromagnetic force, it is not entirely ruled out. Models with so-called milli-charged dark matter where (e.g. via kinetic mixing) dark matter has a highly suppressed coupling to the photon are not entirely ruled out. [66]

limit on the neutron electric dipole moment [53, 26]. However, there is no theoretical reason in the Standard Model why θ has to be exceedingly small. This fine-tuning problem is known as the strong CP problem [139]. An elegant solution was proposed in Refs. [124, 123], where θ is promoted to a field that dynamically relaxes to a CP-conserving minimum. This field, called the axion, can be understood as the pseudo Nambu-Goldstone boson arising from the spontaneous breaking of the global $U(1)$ Peccei-Quinn (PQ) symmetry [149, 150]. The axion a dynamically relaxes $\bar{\theta} = \theta - \langle a/f_a \rangle$ to a vanishing value consistent with experiments. A model with a weak scale decay constant f_a was initially proposed [149, 150] but immediately ruled out by laboratory searches. Today, supernovae gives the strongest lower bound giving $f_a \gtrsim 10^8$ GeV [62, 128, 145, 113, 129]. Since the axion is very light and stable on cosmological time scales, one can imagine a scenario where its relic abundance accounts for the observed dark matter (DM) abundance $\Omega_{\text{DM}} h^2 = 0.12$. A thermal axion relic abundance is too hot and scarce to be consistent with cold DM. Two non-thermal production mechanisms are commonly considered.

The relic abundance from the misalignment mechanism [127, 2, 56], namely coherent oscillations due to an initial axion field value $a = \theta_{\text{mis}} f_a$ give an energy density ρ_a via the equations of motion,

$$\ddot{\theta}_a + 3H\dot{\theta}_a = -m_a^2 \sin \theta_a \tag{1.18}$$

$$\rho_a = \frac{1}{2} (m_a^2 a^2 + \dot{a}^2) \tag{1.19}$$

where $\theta_a \equiv a/f_a$ parametrizes the axion field value a and H is the Hubble expansion rate. In the conventional setup where m_a is assumed to be negligible compared to the Hubble parameter during inflation, the axion field value is practically frozen due to a

large Hubble friction term in Eq. (1.18) with the solution approximated by

$$\theta_0 \simeq \theta_i e^{-N_e m_a^2/3H_I^2} \quad \text{for } m_a \ll H_I, \quad (1.20)$$

with θ_0 (θ_i) the angle at the end (onset) of inflation, unless the number of e-folding is exceedingly large $N_e \sim (H_I/m_a)^2$ as pointed out by Refs. [55, 74, 142]. As a result of inflation, the misalignment angle takes a random but uniform value θ_{mis} in the observable universe. Around the QCD phase transition, the axion acquires a mass from the QCD non-perturbative effects and starts to oscillate, when $3H \simeq m_a$, from $a_{\text{mis}} = \theta_{\text{mis}} f_a$ towards the minimum today. Without fine-tuning, θ_{mis} is expected to be order unity. The coherent oscillations of axions contribute to the cold dark matter abundance

$$\Omega_a h^2 = 0.12 \langle \theta_{\text{mis}}^2 \mathcal{F}(\theta_{\text{mis}}) \rangle \left(\frac{f_a}{5 \times 10^{11} \text{GeV}} \right)^{7/6}, \quad (1.21)$$

where $\mathcal{F}(\theta_{\text{mis}}) \simeq 1$ for $\theta_{\text{mis}} \ll \pi$ and, for $\theta_{\text{mis}} \gtrsim 0.9\pi$, is analytically approximated by [109]

$$\mathcal{F}(\theta_{\text{mis}}) \simeq \frac{16\sqrt{2}}{\pi^3} \left[\ln \left(\frac{1}{1 - \theta_{\text{mis}}/\pi} \right) \right]^{7/6}. \quad (1.22)$$

The exponents in Eqs. (1.21) and (1.22) assume the topological susceptibility of QCD given by the dilute instanton gas approximation (see the lattice results in Refs. [125, 34, 40, 33, 73]) but our results are insensitive to this uncertainty. With the natural assumption of $\mathcal{O}(1)$ initial misalignment, $f_a = 10^{11} - 10^{12}$ GeV is compatible with the observed DM abundance. If the PQ symmetry is broken after inflation and the domain wall number is unity, the abundance of axions emitted from the string-domain wall network is [54, 98, 104]

$$\Omega_{\text{string,DW}} h^2 \simeq 0.04 - 0.3 \left(\frac{f_a}{10^{11} \text{GeV}} \right)^{7/6}. \quad (1.23)$$

The decay constant $f_a \sim 10^{11}$ GeV reproduces the DM abundance.

As ongoing axion experiments are about to reach sensitivity required to probe small decay constants of $10^8 \text{ GeV} < f_a < 10^{12} \text{ GeV}$ [148, 21, 19, 133, 42, 23, 70, 136, 22, 29, 58], exploring the theoretical landscape pertaining to small f_a is important. Some studies have been successful in allowing small f_a in a natural setting, such as parametric resonance from a PQ symmetry breaking field [51] and decays of quasi-stable domain walls [87, 88, 98, 81]. The misalignment mechanism can reproduce the observed DM abundance for $f_a \ll 10^{12} \text{ GeV}$ if θ_{mis} is taken sufficiently close to π [144, 109, 137, 25, 147], where the anharmonicity factor $\mathcal{F}(\theta_{\text{mis}})$ becomes important.

It is also theoretically interesting to consider a decay constant above the grand unification scale $M_{\text{GUT}} \simeq 2 \times 10^{16} \text{ GeV}$, which is a typical prediction of string theory [138]. It is also motivated from the field theory point of view in the supersymmetric Standard Model. The breaking of the PQ symmetry may be of the same origin as the breaking of grand unification [151, 117, 78]. Actually, in four dimensional grand unified theories, if the μ term of the Higgs doublets is controlled by the PQ symmetry, as is the case with the DFSZ model [57, 154], the symmetry breaking scale must be around the unification scale [72, 153, 80]. Many experimental efforts have since been devoted to this mass range of axions [39, 92, 120]. Nevertheless, ultralight QCD axions are subject to overproduction of dark matter from the misalignment mechanism.

CHAPTER II

Yukawa Couplings in the String Landscape

In this chapter we will describe the work done to explore the string landscape of M-theory on manifolds of G_2 Holonomy. We will begin by introducing the M-theory framework in Section 2.1. In Section 2.2 we discuss unification of the standard model with a gauged E_8 symmetry. Finally, in Section 2.3 we discuss work done to relate E_8 symmetry breaking parameters to the moduli fields which arise in geometric engineering, as well as the computational methods used to find numerical values consistent with our universe.

2.1 M-theory and Manifolds of G_2 Holonomy

String theory began as an attempt to describe strong interactions [146], and it was later realized that one could describe graviton interactions within this framework [134], paving the way for a quantum theory of gravity with bosonic string theory. Bosonic string theory, however, failed as a phenomenological model because it predicted a critical dimension of 26, tachyonic states, and only contained bosonic states without a method for introducing fermionic states. A resolution to these problems came later with in the form of superstring theory [75]. Adding supersymmetric string states ameliorated the problem by removing tachyonic states, introducing fermionic states, yet demands a critical dimension to $D = 10$. M-theory with a critical dimension

$D = 11$ was introduced [152], and has shown increasing promise as a fundamental UV complete theory [5, 15, 11, 7, 8, 14, 6, 9, 12, 10, 13, 4, 3, 3, 93, 95, 94, 63].

We are interested in string theory constructions whose effective action below the string scale M_{string} is $D = 4$ with $\mathcal{N} = 1$ supersymmetry. To achieve such a theory, we factorize the background geometry of spacetime to $\mathbf{M}_4 \times \mathbf{X}_7$ where \mathbf{M}_4 is Minkowski space and \mathbf{X}_7 is a compact space. Each point in $\mathbf{M}_4 \times \mathbf{X}_7$ is locally 11d with a set of 11d spinor supercharges. For a supersymmetry to be preserved upon compactification, the corresponding supercharge must be well defined globally on $\mathbf{M}_4 \times \mathbf{X}_7$. Since \mathbf{X}_7 is curved, parallel transport of a spinor about a closed loop will, in general, impose a non-trivial transformation. To preserve supersymmetry, we must find a manifold whose spin connection permits a Killing spinor ξ where

$$\nabla_m \xi(x^m) = 0. \tag{2.1}$$

with covariant derivative on \mathbf{X}_7 , ∇_m . This requirement is directly related to the holonomy group of a manifold, which is the set of all transformations of ξ under parallel transport. For a seven dimensional manifold, the only manifolds that leave one supersymmetry unbroken are those of G_2 holonomy.

A seven dimensional manifold with these properties is given by the fibration of $\widehat{\mathbb{C}^2/\Gamma_{\text{ADE}}}$ over a base space M_3 . The space Γ_{ADE} is an asymptotically local Euclidian (ALE) manifold with a singularity at the origin. The structure of the singularity is rich in that it permits an effective theory with non-Abelian ADE gauged symmetries. The type of singularity for a given subgroup Γ_{ADE} can be found by resolving the singularity at the origin via the process of so-called ‘blowing up’.

Resolving a singularity amounts to expanding the fixed point into a projective space $\mathbb{P}^1(\mathbb{C})$. After the first blowing-up, we may still find singularities in the projective space \mathbb{P}^1 , and to correctly classify the singularity we repeat the blowing-up process

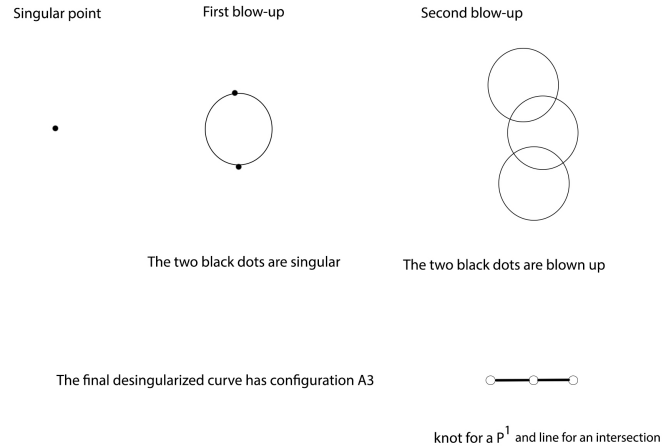


Figure 2.1: An A_3 type singularity being fully resolved will have a configuration of three Riemann spheres $\mathbb{P}^1(\mathbb{C})$ which intersect according to A_3 Dynkin diagram.

until there are no more singularities to resolve. The result is a set of intersecting sub-manifolds \mathbb{P}^1 , with the intersection pattern corresponding to the Dynkin diagram of the symmetry group.

Figure 2.1 gives a pictorial illustration of a singularity of type A_3 . Each of the consequent \mathbb{P}^1 can be called a two-cycle. So, a singularity of type A_3 is one that, when completely resolved, has a configuration of A_3 . Similarly, a singularity of a certain Dynkin diagram has the blown-up configuration of that diagram. The explicit diagrams with the associated group are in Figure 2.2.

We have seen that the 2-cycles \mathbb{P}^1 directly relate to the smoothing of singularities. We can use the volume of the 2-cycles to parametrize the resolution. Such a method of smoothly parametrizing the blowing-up is called deformation.

For each 2-cycle, we use a harmonic one-form ϕ on M_3 , which can be thought of as a metric-invariant 3-vector field on M_3 , to parametrize the size of the 2-cycle. Alternatively, Katz et al [36, 97] use the coefficients in the Cartan subalgebra as the parameters. Consistently, there is a one-to-one bijection between the two parametrizations given

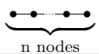
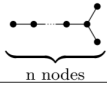
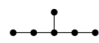
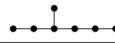

Type	diagram	finite subgroups of $SU(2)$	simple Lie group
A_n		\mathbb{Z}_{n+1}	$SU(n+1)$
D_n		$2\mathbb{D}_{2(n-2)}$	$SO(2n), Spin(2n)$
E_6		$2T$	E_6
E_7		$2O$	E_7
E_8		$2I$	E_8

Figure 2.2: Dynkin diagram and associated groups.

by Table 2.1. Following the existing literature, we denote $\widehat{G}(f_1, f_2, f_3, \dots, f_n)$ as the family of $\widehat{\mathbb{C}^2}/\Gamma_G$ parametrized by the coordinates f_i in Cartan subalgebra where n is the rank of G and use Table 2.1 to compute the “volume” one-form ϕ when needed ¹.

The construction of M theory compactified on a circle is dual to type IIA string theory. Specifically, when a M2 brane wraps around one of the basis two cycles of the resolved E_8 singularity in our model, it is dual to a string wrapping around a circle in type IIA. When the moduli in our theory go to infinity, it is equivalent to the volume of the two cycles going to infinity. This is dual to the infinite radius limit of a circle in type IIA [119].

2.2 E_8 Unification

Our goal is to describe all the particles by resolving one single ADE singularity. E_8 is the only simple Lie group that does the job. E_8 and its breaking have been studied by several authors [111, 47, 35, 122, 59, 41, 71, 64, 121]. Unification under an E_8 gauge symmetry is an attractive solution because it can account for all observed particles

¹More details on root system and deformation are in [96].

	Positive Roots of E_n	Volume of Corresponding Two-Cycle
	$e_i - e_{j>i}$	$f_i - f_{j>i}$
	$-e_0 + e_i + e_j + e_k$	$f_i + f_j + f_k$
$n \geq 6$	$-2e_0 + \sum_{j=1}^6 e_j$	$\sum_{j=1}^6 f_j$
$n=8$	$-3e_0 + e_i + \sum_{j=1}^8 e_j$	$f_i + \sum_{j=1}^8 f_j$

Table 2.1: Positive roots of E_n and the associated one-forms (sometimes called “area” in literature) controlling the sizes of 2-cycles on the ALE fiber.

and families. For example, one symmetry breaking path is $E_8 \rightarrow SU(3) \times E_6$ in which case the adjoint field of E_8 breaks into the adjoint of E_6 , **27**, and fundamental of $SU(3)$ **3**, giving three copies of the **27**, one for each family. The **27** of E_6 has enough matter content to account for all quarks, leptons, bosons we currently observe in addition an extra Higgs (as required by the MSSM), a right handed sterile neutrino, and other exotic particles.

Let $\widehat{E}_8(f_1, \dots, f_8)$ be the resolution of a E_8 singularity parametrized by deformation moduli f_i 's which are one-forms on M_3 . The simple roots are associated with the volumes of the blown-up 2-cycles by Table 2.1 [36].

Each simple root, or equivalently each knot on the Dynkin diagram, will initially represent a vanishing cycle at the singularity. To break a group to a smaller group, we will “cut” a knot on their diagram so that we get the diagram of the smaller group. Each “cutting” is performed by blowing up the cycle (which was initially vanishing) associated with the knot. We recall that each cycle in the above Dynkin diagram gives rise to a boson whose mass is proportional to the volume of the cycle. Therefore, a vanishing cycle in the above Dynkin diagram will result in a massless boson. The goal is to keep the SM gauge bosons massless (zero volume cycles) while the other bosons are massive (non-zero volume cycles). We will follow the breaking path² of [35]. Figure 2.3 summarizes the above steps. In the figure, we start with an E_8 singularity which corresponds to $\widehat{E}_8(0, 0, 0, 0, 0, 0, 0, 0)$, then turn on the volumes

²Different paths to the same subgroup will lead to the same physics. This is because if there is a diffeomorphism between X_1 and X_2 so that their hyper-Kähler structures agree, then they are isometric.

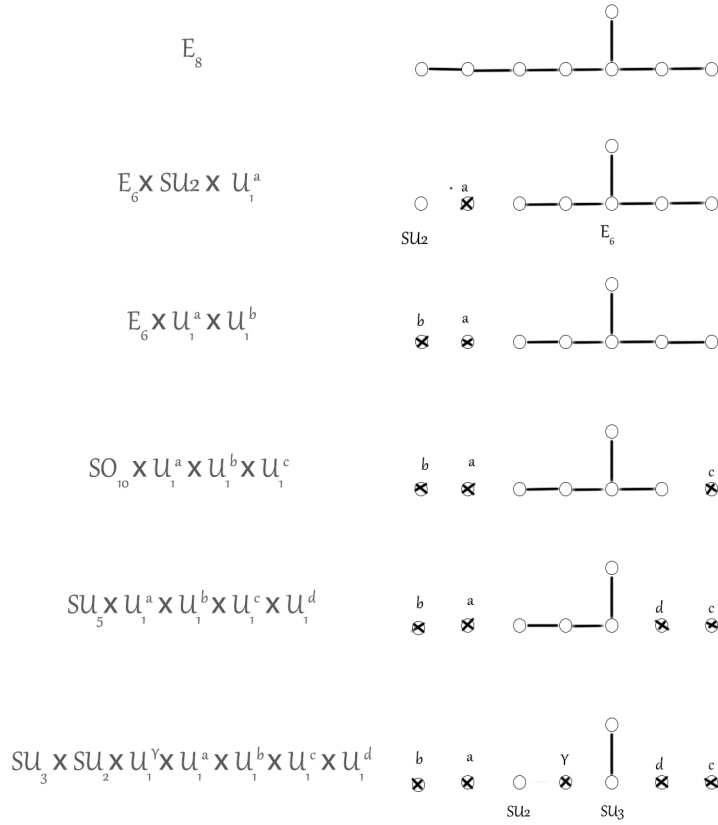


Figure 2.3: Breaking of E_8 by resolving singularity

of the cycles associated with the crossed knots by giving non-zero values for one-form f_i 's. There are five volumes needed to be turned on, so we parameterize f_i 's by five non-zero one-forms a, b, c, d and Y (note that Y here is the one-form associated with hypercharge $U(1)^Y$, not the hypercharge itself). They are simply parameters that are linearly combined in a specific way so that the volumes of the cycles vanish or blow up appropriately by Table 2.1. Then the final manifold is parameterized as in [36]

$$\begin{aligned}
& \widehat{E}_8(a + b + c + d + \frac{2}{3}Y, a - b + c + d + \frac{2}{3}Y, \\
& -c - d - \frac{7}{3}Y, -c - d - \frac{7}{3}Y, -c - d + \frac{8}{3}Y, \\
& -c - d + \frac{8}{3}Y, -c + 3d - \frac{4}{3}Y, 2c - 2d - \frac{4}{3}Y).
\end{aligned} \tag{2.2}$$

We can check each step of Fig. 2.3 by setting all a, b, c, d , and Y in Eq. 2.2 to zero, then turn them on accordingly to each step, and compute the volumes using Table 2.1. In the following, we can check the volumes of the cycles corresponding to the simple roots in the final step

$$\left(\begin{array}{cc}
e_1 - e_2 & 2b \\
e_2 - e_3 & a - b + 2c + 2d + 3Y \\
e_3 - e_4 & 0 \\
e_4 - e_5 & -5Y \\
e_5 - e_6 & 0 \\
e_6 - e_7 & -4d + 4Y \\
e_7 - e_8 & -3c + 5d \\
-e_0 + e_6 + e_7 + e_8 & 0
\end{array} \right) \tag{2.3}$$

This is exactly the configuration of Fig. 2.3. Note that one can use any different set of one-forms as long as they fulfill the desired configuration and sufficiently parameterize the independent non-vanishing cycles. Ultimately, whatever constrain we make, to avoid an unwanted shrunk cycle which will lead to an extra massless boson, we have to make non-zero volumes in the above table remain non-zero. To achieve this, we set the constraints on our parametrization as tabulated in Table 2.2.

Constraint	Root	Broken Subgroup
$b \neq 0$	$e_1 - e_2$	U_1^b
$a - b + 2c + 2d + 3Y \neq 0$	$e_2 - e_3$	U_1^a
$Y \neq 0$	$e_4 - e_5$	U_1^Y
$Y \neq d$	$e_6 - e_7$	U_1^d
$c \neq \frac{5}{3}d$	$e_7 - e_8$	U_1^c

Table 2.2: Constraints required to preserve \mathcal{G}_{SM} and break the other E_8 subgroup symmetries.

2.2.1 Fermion Representations

Given a gauge group H for the theory, the corresponding cycles on the fiber are shrunk everywhere along the base manifold M_3 . Those cycles correspond to the simple roots of H . A matter representation happens at the points where additional cycles associated with positive roots (see Table 2.1) vanish. By letting the positive roots vanish one by one, we can find all the resulting representations. We will do a few examples showing how to calculate the representation.

First, we consider $e_2 - e_3$ cycle. Using the above table, we conclude that the associated volume is $f_2 - f_3 = a - b + 2c + 2d + 3Y$. Now, we consider the curve where this particular cycle vanishes: $a - b + 2c + 2d + 3Y = 0$. In order to know what representation emerges at this curve, we consider what kind of weight diagram is generated from $e_2 - e_3$ and the roots from the gauge group (corresponding to the globally shrunk cycles) $e_3 - e_4$ (corresponding to $SU(2)$), and $e_5 - e_6$ and $-e_0 + e_6 + e_7 + e_8$ (corresponding to $SU(3)$). In more details, we will try to find what are the positive roots we can get from $e_2 - e_3$ by adding or subtracting $e_3 - e_4$, $e_5 - e_6$, and $-e_0 + e_6 + e_7 + e_8$. From above, we see that there are two positive roots corresponding to $SU(2)$, so the particle will behave like $\mathbf{2}$ of $SU(2)$. Only one positive root for $SU(3)$ case, so it is a singlet for $SU(3)$. Thus, this is a $(\mathbf{2}, \mathbf{1})$ of $SU(2) \times SU(3)$ (corresponding to H_2^u as in the Table 2.3). Notice that above calculation implies that $e_2 - e_4$ yields the same particle.

	SU_3	SU_2	U_1^a	U_1^b	U_1^c	U_1^d	U_1^Y
Q_1	3	2	1	1	-1	-1	1
Q_2	3	2	1	-1	-1	-1	1
Q_3	3	2	-2	0	-1	-1	1
u_1^c	$\bar{\mathbf{3}}$	1	1	1	-1	-1	-4
u_2^c	$\bar{\mathbf{3}}$	1	1	-1	-1	-1	-4
u_3^c	$\bar{\mathbf{3}}$	1	-2	0	-1	-1	-4
d_1^c	$\bar{\mathbf{3}}$	1	1	1	-1	3	2
d_2^c	$\bar{\mathbf{3}}$	1	1	-1	-1	3	2
d_3^c	$\bar{\mathbf{3}}$	1	-2	0	-1	3	2
L_1	1	2	1	1	-1	3	-3
L_2	1	2	1	-1	-1	3	-3
L_3	1	2	-2	0	-1	3	-3
H_1^u	$\bar{\mathbf{1}}$	2	1	1	2	2	3
H_2^u	$\bar{\mathbf{1}}$	2	1	-1	2	2	3
H_3^u	$\bar{\mathbf{1}}$	2	-2	0	2	2	3
H_1^d	$\bar{\mathbf{1}}$	2	1	1	2	-2	-3
H_2^d	$\bar{\mathbf{1}}$	2	1	-1	2	-2	-3
H_3^d	$\bar{\mathbf{1}}$	2	-2	0	2	-2	-3
e_1^c	1	1	1	1	-1	-1	6
e_2^c	1	1	1	-1	-1	-1	6
e_3^c	1	1	-2	0	-1	-1	6

Table 2.3: Relevant particles from three families of E_6 .

A complete discussion of this process is present in the literature [36] and the charges for relevant particles in this paper is presented in Table 2.3. The location of the singularity associated with a particle is a linear combination of moduli weighted by the charges. For instance, the location of Q_1 is the curve that satisfies

$$a + b - c - d + Y = 0 \tag{2.4}$$

2.3 Yukawa Couplings from Three-Cycle Volumes

In the superpotential, a cubic term ABC is allowed at tree level if the product transforms as a singlet under the gauge group. In particular, that implies the sum of charges for each of the $U(1)$'s is zero. If such a term happens, each of the particles

$A, B,$ and C will live on a different conical singularity which corresponds to different points $t_A, t_B,$ and t_C on the base W which are solutions of equations derived from Table 2.3 (similar to 2.4). The idea of this section is that the Yukawa coupling coefficient of this term is proportional to the exponential of the volume of the three-cycle wrapping around the three singularities

$$\text{Yukawa coupling} = n_{ABC} \frac{e^{-Vol(\Sigma_{ABC})}}{\Lambda_{ABC}} \quad (2.5)$$

where Σ_{ABC} is the three-cycle wrapping around the singularities, n_{ABC} is the sign of the term which depends subtly on the orientation of the three cycle[37]³, Λ_{ABC} is a scale factor which is approximately the volume of G_2 manifold. We will temporarily ignore both of n_{ABC} and Λ_{ABC} in our analysis in this section.

We are interested in the limit where gravity decouples. The G_2 manifold here is treated as large enough to make the calculation manageable. Then, we can focus on a local patch of M_3 which is approximately \mathbb{R}^3 . The volume of the three-cycle in the linearization has been formulated by [36]. However, a more complete analysis shows the requirement of the harmonic condition and relative rotations of the fields. By BPS equations [37], locally for each moduli ϕ ($\phi = a, b, c, d,$ and Y . These are the f_i 's in the previous sections), there is a harmonic function h_ϕ on M_3 base so that $\phi = dh_\phi$ [37]. For simplicity, we think of ϕ as a three vector, and $\phi = \nabla h_\phi$. The harmonic condition requires that $\Delta h_\phi = 0$, which implies

$$\partial_i \phi^i = 0. \quad (2.6)$$

This requires

$$\phi = Ht + v, \quad (2.7)$$

³Details of how to determine n_{ABC} is in [37] and Appendix F of [68]

where H is a real traceless symmetric 3x3 matrix, v is a real three vector, t is a local real parametrization of the 3d base. Then, h_ϕ will have the form

$$\frac{1}{2}t^T H t + v^T t + c \tag{2.8}$$

where c is a constant term.

The location of a particle, say X , is a zero t_X of a linear combination ϕ_X of a, b, c, d , and Y with by the charges from table 2.3. From previous discussion, t_X is the critical point of a harmonic function h_{ϕ_X} . Assume the critical points are isolated. This is the same as assuming H_X is invertible. The critical point of h_{ϕ_X} or the zero point of ϕ_X is

$$t_X = -H_X^{-1}v_X. \tag{2.9}$$

Then, if the ABC term is allowed, i.e, $h_{\phi_A} + h_{\phi_B} + h_{\phi_C} = 0$, the volume for the three-cycle wrapping the three critical points t_A, t_B and t_C is ⁴

$$\begin{aligned} Vol(\Sigma_{ABC}) &= h_{\phi_A}(t_A) + h_{\phi_B}(t_B) + h_{\phi_C}(t_C) \\ &= \frac{1}{2}(-v_A^T H_A^{-1}v_A - v_B^T H_B^{-1}v_B \\ &\quad + (v_A + v_B)^T (H_A + H_B)^{-1}(v_A + v_B)). \end{aligned} \tag{2.10}$$

Notice that the constant c in equation (2.8) plays no role here due to cancellation, so in practice, we will simply drop it. In section 2.4.3, explicit computation for a Yukawa coupling is shown for a quark term.

⁴[37] gives formulation for the general case, which has been applied to this linear case.

2.4 Quark Terms

2.4.1 General Quark Terms

Recall that the quarks get mass when the Higgses receive VEVs. For example,

$$\lambda^{ij} H_k^u Q_i u_j \rightarrow \langle H_k^u \rangle \lambda^{ij} Q_i^k u_j^k. \quad (2.11)$$

Ellis et al [63] showed that $\tan \beta \approx 7$, from electroweak symmetry breaking, so we know both up and down VEVs in the two-Higgs-doublets model. We will discuss later how to adapt these into the six Higgs doublets in this paper. Quark terms that satisfy vanishing sum of charges are

$$\begin{aligned} & Q_1 u_2^c H_3^u + Q_2 u_1^c H_3^u + Q_1 d_2^c H_3^u + Q_2 u_1^c H_3^u + \\ & Q_2 u_3^c H_1^u + Q_3 u_2^c H_1^u + Q_2 d_3^c H_1^u + Q_3 u_2^c H_1^u + \\ & Q_3 u_1^c H_2^u + Q_1 u_3^c H_2^u + Q_3 d_1^c H_2^u + Q_1 u_3^c H_2^u. \end{aligned} \quad (2.12)$$

Note that there is no diagonal term in this general setting. Also, some couplings between the Higgs and the quarks which could have been possible in SM are forbidden here due to the extra $U(1)$'s. Nonetheless, those terms can still be generated by Giudice-Masiero mechanism after the breaking of supergravity [43, 3]. However, we will leave this mechanism to future study in the context of M-theory with E_8 orbifold. In the following sections, we will focus on the simplest constraints on the moduli to make the theory physical.

The relevant terms for leptons are

$$L_1 e_2^c H_3^d + L_2 e_3^c H_1^d + L_3 e_1^c H_2^d + \quad (2.13)$$

$$L_1 \nu_2^c H_3^u + L_2 \nu_3^c H_1^u + L_3 \nu_1^c H_2^u. \quad (2.14)$$

Notice that we only have Dirac mass terms here. Majorana terms may require quartic level, extra particles getting a VEV, or extra constraints on the moduli, so we will not discuss such terms in this paper.

2.4.2 Diagonal Terms and Setting $a = 0$

Equation 2.12 shows that there is no diagonal term for the quark matrices. This appears to be a problem because with the top quark mass much larger than those of up and charm quarks, the trace of the mass matrix must be non-zero. This problem is generic in our method of constructing three families from E_8 singularity. The same issue was discussed in the F-theory context in [30]. The reason for this is the conservation of charge in a and b . Hence, this directly relates to the separation of families because a and b break the adjoint of E_8 into three $\mathbf{27}'$ s in E_6 . So, particles in the same family must have the same charge in a and b , making it impossible for them to form a singlet cubic term within the same family in generic setting. One way to remedy this is to introduce a self intersecting curve for the up-type when $Y = 0$ [30], using the fact that in grand unified theories u and Q both stay on the same curve of $\mathbf{10}$ of $SU(5)$. However, this method cannot be applied for down-type as d does not stay on the same curve as Q . Moreover, self-intersecting requires higher order than linearization which we will not pursue here. Alternatively, Bourjaily et al [36] also discuss the contribution of quartic terms. This will require giving large VEVs for extra particles, creating more parameters which we will not consider at this time.

In this paper, we can consider some constraint on a and b leading to possible non-zero diagonal terms. This in essence sets a relation for a and b charges. We still keep in mind the condition of non-vanishing volumes in (2.3) as we do not wish to unnecessarily enhance the gauge symmetry. The simplest constraint we can make is $a = 0$. Although it is intriguing to study other constraints, we will ignore them in this paper. This constraint will restrict the gauge group to $SU(3) \times SU(2) \times U(1)^Y \times U(1)^b \times U(1)^c \times$

$U(1)^d$. In term of geometry, this breaking of $U(1)^a$ is equivalent to restricting the basis 2-cycles in a linear relation, reducing the number of independent 2-cycles and hence number of $U(1)$'s.

2.4.3 Quark Mass Matrices

After setting $a = 0$ together with the localization, the up-type quark mass matrix can be computed. We will show one example of the computation here for $M_{12}^u u_1 u_2^c$. It comes from the term

$$\lambda_{123}^u Q_1 u_2^c H_3^u. \quad (2.15)$$

When the Higgs gets VEV at low scale, the term becomes

$$\lambda_{123}^u \langle H_3^u \rangle u_1 u_2^c, \quad (2.16)$$

where $M_{12}^u = \lambda_{123}^u \langle H_3^u \rangle$. Then, all that is left is to compute λ_{123}^u . At high scale, λ_{123}^u can be calculated from (2.10) and Table 2.3. In the linearization language

$$H_{Q_1} = H_b - H_d + H_Y \quad (2.17)$$

$$v_{Q_1} = v_b - v_d + v_Y \quad (2.18)$$

$$H_{u_2} = -H_b - H_d - 4H_Y \quad (2.19)$$

$$v_{u_2} = -v_b - v_d - 4v_Y \quad (2.20)$$

then (2.10) gives

$$Vol\{\Sigma_{Q_1 u_2^c H_3^u}\} = \tag{2.21}$$

$$\begin{aligned} & \frac{1}{2} \left((v_b - v_d + v_Y)^T (H_b - H_d + H_Y)^{-1} (v_b - v_d + v_Y) + \right. \\ & (-v_b - v_d - 4v_Y)^T (-H_b - H_d - 4H_Y)^{-1} (-v_b - v_d - 4v_Y) + \\ & \left. (2v_d + 3v_Y)^T (+2H_d + 3H_Y)^{-1} (2v_d + 3v_Y) \right) \end{aligned} \tag{2.22}$$

Thus, (2.5) , ignoring the overall scaling, gives

$$\begin{aligned} \lambda_{123}^u = n_{12}^u \exp \left\{ \right. \\ & - \frac{1}{2} \left| (v_b - v_d + v_Y)^T (H_b - H_d + H_Y)^{-1} (v_b - v_d + v_Y) + \right. \\ & (-v_b - v_d - 4v_Y)^T (-H_b - H_d - 4H_Y)^{-1} (-v_b - v_d - 4v_Y) + \\ & \left. (2v_d + 3v_Y)^T (+2H_d + 3H_Y)^{-1} (2v_d + 3v_Y) \right| \left. \right\} \end{aligned} \tag{2.23}$$

Then, we have to run these Yukawa couplings down to the SM scale to compute the mass. Note that for the diagonal term $Q_3 u_3^c H_3^c$, obtained from setting $a = 0$, can be computed by the above method.

2.4.4 Six Higgs VEVs

In the six Higgs doublets model without extra $U(1)$'s, one can choose a basis for up-type and down-type Higgses so that only one pair of Higgses gets a VEV without loss of generality. Here, due to different charges for the Higgses from the extra $U(1)$'s (see Table 2.3), we cannot make such a choice of basis.

We will try to translate from the two VEVs of SM Higgses to the six VEVs in our theory. By standard QFT, we can relate this by looking at the mass of W boson in

the SM and identify

$$\langle H_u^{SM} \rangle^2 = \sum_i \langle H_u^i \rangle^2, \quad (2.24)$$

$$\langle H_d^{SM} \rangle^2 = \sum_i \langle H_d^i \rangle^2. \quad (2.25)$$

So, we can use spherical parametrization to write

$$\begin{aligned} \langle H_{u/d}^1 \rangle &= \langle H_{u/d}^{SM} \rangle \cos \phi_{u/d} \sin \theta_{u/d}, \\ \langle H_{u/d}^2 \rangle &= \langle H_{u/d}^{SM} \rangle \sin \phi_{u/d} \sin \theta_{u/d}, \\ \langle H_{u/d}^3 \rangle &= \langle H_{u/d}^{SM} \rangle \cos \theta_{u/d}. \end{aligned} \quad (2.26)$$

Such Higgs VEVs can lead to flavor changing neutral currents (FCNC). We keep the mixing angles small and assume no problems with FCNC, which implies $\theta \ll 1$.

Note that the Yukawa couplings in M-theory belong to the high energy scale. We will attempt to use the already existent list of high scale Yukawa coupling running from SM experimental Yukawas in Table 1 of [24]⁵ and find a solution for our parameters. We assume the effect of the extra U(1)'s from our theory in the renormalization group equations (RGEs) is not significant, and the Yukawas have approximately the same magnitudes as in [24].

In order to compare with physical Yukawa couplings, we need to take into account a few modifications. First, as mentioned in [30], we need a scaling factor to normalize the wave function. For cubic Yukawa, it is roughly proportional to $V_{G_2}^{-\frac{1}{2}}$ where V_{G_2} is the volume of G_2 manifold and still a parameter in our theory (as local model cannot determine the global volume). The scaling factor for all the cubic Yukawas is a parameter in this local model.

⁵The *GUT* group is slightly different, but we assume the magnitude of the couplings are approximately the same. See also [131].

2.4.5 Higgs VEVs

One the other hand, recall that the Higgses only get VEVs at low scale. Therefore, precisely speaking, we can only consider the VEVs of the six Higgses after we run our M-theory Yukawa couplings down to low scale. Unfortunately, at high scale, we only have a set of algebraic expressions for M-theory Yukawas, making the running down to low scale complicated. Moreover, we cannot directly fit our Yukawas with the existing data of high scale running from SM Yukawas because they all assume a two Higgses model. Therefore, to remedy this problem, we will use a heuristic treatment assuming that the angular factors, in equations (2.26), are regarded as part of the low scale Yukawa couplings and do not change much while running to high scale. Then, the effective VEVs at low scale are just the two VEVs from the SM, and the Yukawa couplings at high scale used to fit with Table 1 of [24] then are

$$Y = f(\phi, \theta)\lambda \tag{2.27}$$

where λ is a Yukawa computed from section 2.4.3 and $f(\phi, \theta)$ is one of the angular functions associated with the Higgs fields from equations (2.26.)

2.5 Yukawa matrix for gauge group $SU(3) \times SU(2) \times U(1)^Y \times U(1)^b \times U(1)^c \times U(1)^d$

First, we need to fix all extra degrees of freedom. Translation allows setting $v_d = 0$. We also have three degrees of rotation and one degree of scaling to make $v_b = (1, 0, 0)$.

Second, we will try to consider the scattering around special cases of H_b and H_d . Notice from the list in (2.3) that by setting all parameters to zero except b , we see that volumes of root $e_1 - e_2$ and $e_2 - e_3$ are controlled by b . They are responsible for breaking the adjoint of E_8 into three $\mathbf{27}$'s of E_6 (see Figure 2.3), hence are also

responsible for separating the three SM families.

On the other hand, d controls $e_2 - e_3$, $e_6 - e_7$, and $e_7 - e_8$. The blown-up two-cycle of $e_2 - e_3$ breaks the adjoint of E_8 into two $\mathbf{27}$'s of E_6 , which transform as the fundamental and singlet of $SU(2)$ respectively, i.e. $(\mathbf{27}, \mathbf{2}) \oplus (\mathbf{27}, \mathbf{1})$. Thus d separates one family (the top quark family) from the other two in the adjoint of E_8 . The latter still has an $SU(2)$ family symmetry (which is broken when we turn b on). Additionally, $e_6 - e_7$ corresponds to breaking the $\mathbf{27}$'s of E_6 into the presentations of $SO(10)$, separating the Higgses from quarks and leptons. Finally, $e_7 - e_8$ splits the $\mathbf{16}$'s of $SO(10)$ into the $\mathbf{10}$ and $\bar{\mathbf{5}}$ of $SU(5)$. Thus, d also separates the up-type quarks (up, charm, top) from the down-type quarks (down, strange, bottom), i.e. an isospin breaking effect.

2.6 Computational Setup

To estimate moduli parameters Φ compatible with accepted Yukawa coupling measurements \hat{Y} we performed a stochastic gradient descent to minimize the cost function,

$$C(Y(\Phi)) = \sum_{i=1}^9 \frac{\left(\hat{Y}_i - Y_i(\Phi)\right)^2}{\sigma_{\hat{Y},i}} \quad (2.28)$$

where $Y(\Phi)_i$ are the predicted fermion Yukawa couplings for a set of input moduli Φ . The index i runs over all quark and electron-type lepton flavors and the quantities \hat{Y}_i and $\sigma_{\hat{Y},i}$ represent the measured value and corresponding uncertainty for the i th fermion flavor, respectively. The work done in [131] gives estimates for Yukawa couplings at the GUT scale (and their uncertainties) by running measurements tabulated in the Particle Data Group review [157] to a unification scale based on SUSY parameters. The values used in this study are show in Table 2.4.

Custom code was written in `python` to accept parameters Φ and return predictions for the Yukawa couplings Y_i based on the calculations of Yukawa matrices in

Fermion Flavor	\hat{Y}_i	$\sigma_{\hat{Y}_i}$
Top	0.48	± 0.02
Charm	0.0012	± 0.001
Up	3.2×10^{-6}	$\pm 8 \times 10^{-7}$
Bottom	0.051	± 0.002
Strange	9.7×10^{-4}	$\pm 1.1 \times 10^{-4}$
Down	4.9×10^{-5}	$\pm 9 \times 10^{-6}$
Tau	0.070	± 0.003
Muon	0.0041	± 0.0002
Electron	2.0×10^{-5}	$\pm 1 \times 10^{-6}$

Table 2.4: GUT scale Yukawa couplings from [131].

Section. 2.4.3.

2.7 Numerical Evaluation

To test the compatibility of this model with the Standard Model, we perform a regression on the free parameters by a least squares approach. Our calculations of Yukawa couplings are compared to experimentally measured weak scale Yukawa couplings which have been run up to the GUT scale ⁶. The theoretical uncertainty in the calculation dominates over the experimental uncertainties and we only consider theoretical uncertainty when minimizing the sum of the residuals.

Using previous arguments, we set the base parameters corresponding to $a = 0$ to zero, v_d to zero, and v_b to $(1, 0, 0)$. With three 3×3 traceless symmetric matrices H_ϕ and two 3-vectors, we have 18 free parameters from the base space. We have four additional parameters from the Higgs VEVs, satisfying $\langle (H_1^2 + H_2^2 + H_3^2)^{1/2} \rangle = \langle H_{\text{MSSM}} \rangle$. Although we have more free parameters than constraints from the data, the non-linearity in calculating the Yukawas restricts the solutions. A list of numerical solutions is in Appendix. Exploration of the parameter space shows a large scarcity in the number of viable solutions. Many months of computation time were required to find the one viable solution presented in this dissertation. This difficulty lies in

⁶See also [131].

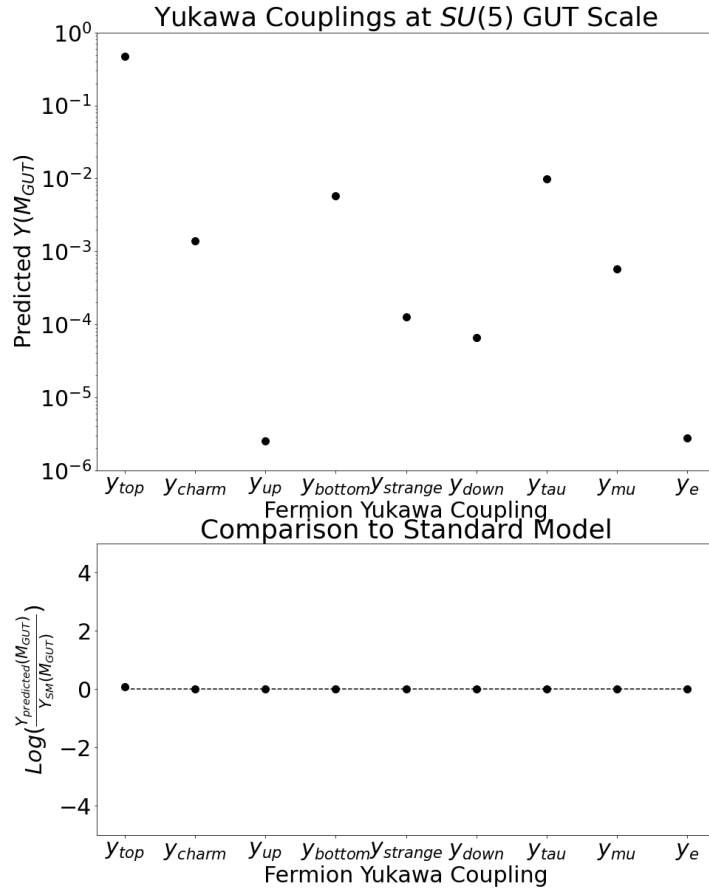


Figure 2.4: A set of sample solutions found numerically. The three symbols indicate three different solutions, and the line indicates the measured value for each Yukawa coupling.

the smoothness of the parameter space. The highly non-linear relation between the parameters and Yukawa couplings lead to many local minima of varying sizes. Without being able to estimate the size of the local minima troughs, we could not easily find a fixed value for the gradient step size to avoid getting stuck in large-width minima while being sensitive to small-width minima.

A set of samples from numerical evaluation is shown in Fig. 2.4. We have observed some general trends among the numerical solutions. Most importantly, there exists a hierarchy of Yukawas within each family which come from the breaking of the flavor and family symmetries. There is a large top quark Yukawa coupling. Finally, it appears that the hierarchy solution only happens when θ is small, an observation that is expected from the aforementioned no-neutral-current condition.

CHAPTER III

Axions Dynamically Driven to the Hilltop

3.1 Introduction

As ongoing axion experiments are about to reach sensitivity required to probe small decay constants of $10^8 \text{ GeV} < f_a < 10^{12} \text{ GeV}$ [148, 21, 19, 133, 42, 23, 70, 136, 22, 29, 58], exploring the theoretical landscape pertaining to small f_a is important. Some studies have been successful in allowing small f_a in a natural setting, such as parametric resonance from a PQ symmetry breaking field [51] and decays of quasi-stable domain walls [87, 88, 98, 81]. The misalignment mechanism can reproduce the observed DM abundance for $f_a \ll 10^{12} \text{ GeV}$ if θ_{mis} is taken sufficiently close to π [144, 109, 137, 25, 147], where the anharmonicity factor $\mathcal{F}(\theta_{\text{mis}})$ becomes important.

In this study, we propose a scenario which dynamically predicts $\theta_{\text{mis}} \simeq \pi$ and thus small f_a in the context of axion DM from the misalignment mechanism. It is commonly assumed that no misalignment angles are special in the early universe, and $\theta_{\text{mis}} \simeq \pi$ requires a fine-tuned initial condition. This is not the case given two conditions are met: 1) the axion field dynamically relaxes to the minimum of the potential in the early universe and 2) the model possesses a non-trivial prediction between the minima of the axion potential in the early and today's epochs. We refer to the axion relaxation with the fulfillment of these requirements as Dynamical Axion Misalignment Production (DAMP). We study DAMP by the dynamics of the Higgs

fields during inflation. The mechanism follows from suspending the assumption that axion's late-time dynamics is agnostic to inflationary dynamics. To be concrete, we study the Minimal Supersymmetric Standard Model (MSSM). The Higgs fields H_u and H_d in general couple to the inflaton potential energy via higher dimensional operators, which lead to so-called Hubble induced masses. The Higgs fields can acquire a large field value in the early universe by virtue of the Hubble induced mass. This large field value gives large quark masses, which enhance the confinement scale to Λ'_{QCD} during inflation. Since m_a is proportional to Λ'_{QCD} , this raises the axion mass to allow for earlier relaxation to the minimum. Note that we need to assume the Higgs fields are not charged under PQ symmetry; otherwise, the decay constant will be as high as the Higgs VEV and suppress the axion mass. For context, early studies [60, 27, 46] have made use of moduli fields to raise the QCD confinement scale $\Lambda_{\text{QCD}} \rightarrow \Lambda'_{\text{QCD}}$ during inflation. This avoids fine-tuning problems that arise under the assumption of an $\mathcal{O}(1)$ initial misalignment with large values $f_a > 10^{12}$ GeV. Later studies [91, 45] used Higgs fields as the moduli fields and refined the scope of the mechanism to reduce isocurvature perturbations for models with large inflation scales, which comes at the cost of an inability to suppress the axion abundance. This loss of abundance predictability is because no assumptions are made about the evolution of the axion minimum through inflation. In the MSSM for example, we have [46]

$$\theta_{\text{eff}} = \theta_{\text{QCD}} + \arg(\det \lambda_u \lambda_d) + 3 \arg(m_{\tilde{g}}) + 3 \arg(B\mu), \quad (3.1)$$

where λ_u, λ_d are the Yukawa coupling matrices, $m_{\tilde{g}}$ denotes the gluino mass, and $B\mu$ is the soft breaking mass for Higgs scalars. Although a large Λ'_{QCD} can help fulfill the first DAMP criterion, we should also explain how a Hubble induced mass fits in with Eq (3.1) to fulfill the second criterion.

The Kähler potential can give rise to a Hubble induced $B\mu$ term. If the argument

of the term is different from the vacuum $B\mu$ term by π and dominates, a shift of π relative to the vacuum value is induced in the axion potential.¹ The difference of π in the arguments can be understood by the (approximate) CP symmetry of the theory, such that the $B\mu$ terms are real and the difference of π is simply the opposite signs of the terms. An approximate CP symmetry is also invoked in Ref. [27], where a relaxation to $\theta_{\text{mis}} \simeq 0$ is considered. Note that the shift of π in the axion potential occurs only if the number of generations is odd.

A large m_a allows the axion field to relax to the bottom of the potential during inflation, and a π shifted axion potential means this minimum coincides with today's hilltop. Without additional particles beyond the MSSM, Λ'_{QCD} and consequently m_a cannot be arbitrarily large; we find $m_a \lesssim 10$ TeV. Thus, in the minimal scenario, we consider TeV scales for Hubble during inflation H_I to allow for the relaxation of the axion misalignment during inflation. We also explore non-minimal models where m_a and thus H_I can be larger. Relaxing the axion arbitrarily close to today's hilltop may cause overproduction of axion DM, but we find that the running of Yukawa terms in the Standard Model (SM) gives a sufficient CP phase change $\mathcal{O}(10^{-16})$ to avoid the scenario [61, 102]. An exciting implication of this mechanism is that f_a is fixed to roughly 3×10^9 GeV by the observed DM abundance and CP-violating phase renormalization in the theory. We impose CP symmetry in the Higgs and inflaton sectors. Additional CP violation (CPV) of up to $\mathcal{O}(10^{-4})$ only induces $\mathcal{O}(1)$ changes in the prediction of f_a . In summary, by the inflationary dynamics of the Higgs fields as well as the (approximate) CP symmetry, we can fulfill both criteria of a DAMP scenario; in particular in this paper we explore the case where the inflationary minimum is shifted by π from today's minimum, which is referred to as DAMP $_{\pi}$.

We now elaborate on the approximate CP symmetry. Although the $\mathcal{O}(1)$ amount of CPV measured in the SM must be generated in the theory, a small CPV in the

¹The case where the arguments are the same is explored in [49] and discussed in IV.

extended sectors can be a consequence of the suppressed couplings with the source of CP violation. Such hierarchical couplings can result from the protection of additional symmetries or the geometric separation in the extra dimensions. Additionally, any quantum corrections that attempt to transfer $\mathcal{O}(1)$ CPV from the SM to the extended sectors are automatically small. The reason is that the CP phase of the Yukawa couplings only becomes physical when all three generations are involved, suggesting that the interactions are suppressed by small Yukawa couplings, mixing among generations, and higher loop factors.² With this CP structure, the implications for the extended sectors are as follows. The (approximate) CP symmetry treats the CP-odd and CP-even moduli differently in such a way that the moduli affecting the axion minimum can be stabilized at the CP-conserving points. The smallness of the CP phases is also guaranteed in the masses of any additional colored particles that we introduce in the non-minimal models. Crucially, a CP symmetry only ensures all relevant parameters are real but does not forbid the change of signs throughout the evolution; this is exactly what can give rise to a shift of π in the axion potential.

In Sec. 3.2 we show how a Hubble induced mass for the Higgs in the early universe can induce an axion mass enhancement and a phase shift of π in the axion potential, fulfilling the DAMP $_{\pi}$ criteria. In Sec. 3.3 we discuss both a set of minimal models with the cosmology fully evaluated, and extended models with a larger viable parameter space and a simplified discussion of the post-inflationary cosmology.

3.2 Dynamical Axion Misalignment Production at the Hill-top

We would like to show that allowing H_u and H_d to acquire large VEVs during inflation can lead to a DAMP $_{\pi}$ scenario. To guide the reader, we first restate the

²Even though the CP symmetry is a solution to the strong CP problem alternative to the axion, the $\mathcal{O}(1)$ CPV in the Yukawa sector may unacceptably modify the θ term. For models that avoid such consequences, refer to Refs. [116, 28, 31, 85]

conditions under which the DAMP model is applicable: 1) the axion field dynamically relaxes to the minimum of the potential in the early universe and 2) the model possesses a non-trivial prediction between the minima of the axion potential in the early and today's epochs. Throughout our discussion of DAMP $_{\pi}$ models, we have in mind a minimal model as a proof of principle and extended models to further explore viable parameter space. Generically, we can include inflaton-Higgs dynamics with the effective operators suppressed by the cutoff scale M in the Kähler potential

$$\Delta K = \frac{|X|^2}{M^2} \left(|H_u|^2 + |H_d|^2 - (H_u H_d + c.c.) - \frac{|H_u|^2 |H_d|^2}{M^2} - \frac{|H_u|^4}{M^2} - \frac{|H_d|^4}{M^2} \right), \quad (3.2)$$

where X is the chiral field whose F -term provides the inflaton potential energy. We omit $\mathcal{O}(1)$ coupling constants here and hereafter. For illustration purposes, we only show lower dimensional operators relevant for the following discussion. Higher dimensional operators do not change the discussion.

During inflation, the inflaton F -term gives the Higgs fields Hubble induced terms,

$$\Delta V = c H_I^2 \left(-|H_u|^2 - |H_d|^2 + (H_u H_d + c.c.) + \frac{|H_u|^2 |H_d|^2}{M^2} + \frac{|H_u|^4}{M^2} + \frac{|H_d|^4}{M^2} \right), \quad (3.3)$$

where $c = (M_{\text{Pl}}/M)^2$ and H_I is the Hubble scale during inflation. We assume that the Hubble induced mass terms are negative. They push the Higgs fields in the D -flat direction $|H_u| = |H_d|$ up to the cutoff scale M , and as we will see in the following sections the large Higgs VEVs realize DAMP $_{\pi}$.

3.2.1 Axion Mass During Inflation

Together with the effective terms from the Kähler potential in Eq. (4.5), the MSSM Higgs potential reads

$$\begin{aligned}
 V_{\text{Higgs}} = & (|\mu|^2 + m_{H_u}^2 - cH_I^2) |H_u|^2 + (|\mu|^2 + m_{H_d}^2 - cH_I^2) |H_d|^2 - (B\mu - cH_I^2) (H_u H_d + c.c.) \\
 & + \frac{g^2 + g'^2}{8} (|H_u|^2 - |H_d|^2)^2 + \frac{g^2}{2} |H_u H_d^*|^2 + \frac{cH_I^2}{M^2} (|H_u|^2 |H_d|^2 + |H_u|^4 + |H_d|^4).
 \end{aligned}
 \tag{3.4}$$

We assume that the Higgs sector is nearly CP symmetric, which is anyway required from the limits on the electric dipole moment for TeV scale supersymmetry. See Refs. [20] and [44] for the latest measurement and its implication to supersymmetric theories, respectively. We also assume a CP symmetry in the inflaton-Higgs coupling. The Higgs fields break $SU(2)_L \times U(1)_Y \rightarrow U(1)_{\text{EM}}$ by both the early universe VEV and today's VEV. Parameterizing the Higgs field space in terms of a radial mode $\phi \equiv |H_u| = |H_d|$ along the D -flat direction and an angular mode $\xi = \arg(H_u H_d)$, which is the relative phase of the Higgs fields, allows us to write

$$V \simeq (m_{\text{SUSY}}^2 - cH_I^2)\phi^2 - (B\mu - cH_I^2)\cos(\xi)\phi^2 + \frac{cH_I^2}{M^2}\phi^4,
 \tag{3.5}$$

where we have taken $m_{H_u} \sim m_{H_d} \sim \mu \sim m_{\text{SUSY}}$. The phases of $H_u H_d$ are chosen so that $\xi = 0$ in the vacuum today. The radial mode, for $\sqrt{c}H_I \gtrsim m_{\text{SUSY}}$, acquires a large VEV of order $\phi_i \sim M$. This is clearly seen from minimizing the potential. Assuming that the sign of the Hubble induced $B\mu$ term is opposite to the vacuum one as shown in Eq. (3.5), the phase initially obtains a value during inflation of $\xi = \pi$, while today's value is $\xi = 0$. We discuss the implication of the phase shift in the next subsection and focus this subsection on the large radial direction.³

³In the extended model discussed below, the sign flip of the $B\mu$ is not necessary. The Hubble induced $B\mu$ term is not necessary as long as the vacuum one is larger than H_I^2 .

The large VEV ϕ_i gives quarks very large masses during inflation. In the MSSM, the 1-loop renormalization group equation (RGE) is

$$\mu_r \frac{d}{d\mu_r} \frac{8\pi^2}{g^2} = 3N - F, \quad (3.6)$$

where μ_r is the renormalization scale, $N = 3$ is the gauge group index, and F is the number of active fermions in the theory. Solving the RGE from the TeV scale up to the scale ϕ_i , and from the scale down while pretending that all quarks are above the scale where the gauge coupling diverges, we obtain the fiducial dynamical scale

$$\Lambda_{\text{fid}} = 10^7 \text{ GeV} \left(\frac{\phi_i}{10^{16} \text{ GeV}} \right)^{2/3} \left(\frac{\tan\beta}{1} \right)^{1/3}. \quad (3.7)$$

This is the physical dynamic scale Λ'_{QCD} if all quarks (including the KSVZ quarks [103, 135]) are above the scale. If some quarks are below the scale, the physical dynamical scale Λ'_{QCD} is given by

$$\Lambda_{\text{fid}} = \Lambda'_{\text{QCD}} \times \prod_{m_q < \Lambda'_{\text{QCD}}} \left(\frac{m_q}{\Lambda'_{\text{QCD}}} \right)^{1/9}. \quad (3.8)$$

The axion mass vanishes when the gluino is massless since strong dynamics gives the mass dominantly to the R-axion. The axion mass is hence given by

$$m_a \simeq \frac{1}{4\pi} \frac{m_{\tilde{g}}^{1/2} \Lambda_{\text{fid}}^{3/2}}{f_a}, \quad (3.9)$$

where we assume that the gluino mass is below the physical dynamical scale and that the large Higgs VEV does not break the PQ symmetry. We include the factor of 4π expected from the naive dimensional analysis [110, 69, 108, 52]. Here $m_{\tilde{g}}$ is the RGE invariant one, $m_{\tilde{g},\text{phys}}/g^2$. The holomorphy of the gauge coupling guarantees that we may use the fiducial dynamical scale to evaluate the axion mass. Physically, the

suppression of the fiducial dynamical scale in comparison with the physical dynamical scale takes into account the suppression of the axion mass by light quarks. For the minimal setup where the dynamical scale is raised solely by large Higgs VEVs as in Eq. (4.9),

$$m_a \simeq 30 \text{ GeV} \left(\frac{m_{\tilde{g}}}{\text{TeV}} \right)^{1/2} \left(\frac{\Lambda_{\text{fid}}}{10^7 \text{ GeV}} \right)^{3/2} \left(\frac{3 \times 10^9 \text{ GeV}}{f_a} \right). \quad (3.10)$$

We may raise the dynamical scale further by introducing additional particles. One possibility is to introduce a moduli field whose field value controls the gauge coupling [60, 27, 46, 91, 45, 89], and assume that the moduli field value during inflation raises the gauge coupling constant. Another possibility is to introduce additional $SU(3)_c$ charged fields and assume that their masses are large during inflation as considered in Ref. [91]. A field whose field value controls the masses of the additional particles can be regarded as a moduli field. For N_Ψ pairs of $SU(3)_c$ fundamental chiral fields with a mass M_Ψ and $M_{\Psi,I}$ in the vacuum and during inflation respectively, the dynamical scale is given by

$$\Lambda_{\text{fid}} = 10^7 \text{ GeV} \left(\frac{M_{\Psi,I}}{M_\Psi} \right)^{N_\Psi/9} \left(\frac{\phi_i}{10^{16} \text{ GeV}} \right)^{2/3} \left(\frac{\tan\beta}{1} \right)^{1/3}. \quad (3.11)$$

To achieve the second requirement of the DAMP scenario, CPV phases in $M_{\Psi,I}$ and M_Ψ should be absent. Instead of flipping the sign of the $B\mu$ term, we may flip the sign of the masses of Ψ to achieve DAMP $_\pi$. We will see later in Sec. 3.3 that this dynamical scale cannot be arbitrarily large because of the backreaction of strong dynamics to the Higgs as well as the PQ sector.

Combining Eqs. (3.9) and (3.11) we find that for appropriate values of H_I , the early universe axion mass is large enough for relaxation of the axion field to its minimum. Since the largeness of the dynamical scale Λ'_{QCD} depends on the VEV of ϕ , the decay of the inflaton and proceeding relaxation of ϕ to today's VEV means

that the post-inflationary cosmology is non-trivial. Prior to exploring this complex cosmology, however, we turn our attention to the relative π phase shift of the axion potential.

3.2.2 Shifted Axion Potential

Another consequence of a large Higgs VEV during inflation from the Kähler potential in Eq. (4.5) is that the relative phase between the Higgs fields is shifted by π as can be seen explicitly in Eq. (3.5). The shift of ξ also shifts the minimum of the axion potential: Eq. (3.1) shows a direct connection between the $B\mu$ term and the axion misalignment angle minimum θ_{eff} . Once the inflaton decays or its energy is redshifted and the Hubble induced terms become subdominant, minimization of the potential is achieved for $\xi = 0$. In the extended model discussed in the previous section, the sign flip of the masses of extra quarks Ψ can achieve a similar situation.

The phase shift of the axion potential is not exactly π because of the $\mathcal{O}(1)$ renormalization of Yukawa couplings. Since the CPV from Yukawa couplings manifests as $\mathcal{O}(10^{-16})$ shifts in the axion potential [61, 102], running these couplings from the early large Higgs VEVs to the electroweak scale necessarily induces an $\mathcal{O}(10^{-16})$ shift in the axion potential. We may also add small CPV to the $B\mu$ terms to induce further shift. Even if the shift is as large as $\mathcal{O}(10^{-4})$, the prediction of f_a changes only by an $\mathcal{O}(1)$ factor.

To summarize, a Kähler potential such as the one in Eq. (4.5) gives Higgs fields Hubble induced masses, and the D -flat potential in Eq. (3.5) is minimized at a large Higgs VEV with an opposite phase from today. The π shifted Higgs phase ξ along with the Yukawa coupling renormalization induce a shift in the axion potential by $\pi - \mathcal{O}(10^{-16})$. This sets the scene for a DAMP $_{\pi}$ scenario where the DM abundance is given by Eq. (1.21) and the value of f_a can be predicted using the anharmonicity factor Eq. (1.22).

3.3 Cosmological Evolution

In Sec. 3.2 we demonstrated that, in the early universe, both a large axion mass and a phase shift of π are possible due to a large Higgs VEV with an opposite phase from today. The remaining question is whether there exists a viable cosmology with a consistent evolution between the two periods without spoiling predictions. We first explore the inflationary and post-inflationary constraints in the minimal model, and then later comment on the broader parameter space allowed by extended models.

3.3.1 Minimal Models

The first consistency check we should perform is to ensure the axion mass is larger than Hubble friction during inflation. As extensively noted, for a given cutoff scale M , the large Higgs VEV $\phi_i \simeq M$ determines Λ'_{QCD} and the axion mass during inflation is enhanced. The suppression of the angle by early relaxation can be approximated by Eq. (1.20). As a benchmark point, we require the suppression factor to be $\theta_0/\theta_i = 10^{-4}$ or smaller during the number of e-foldings of 60. This gives an upper bound on the value of H_I , which is shown in the blue regions of Fig. 3.1 with the left (right) panel for $M = M_{\text{GUT}} \equiv 2 \times 10^{16}$ GeV (M_{Pl}) respectively. The blue contours are also shown for $\theta_0/\theta_i = 10^{-16}$. The orange regions reflect a lower bound on the value of H_I from requiring $cH_I^2 > \max(m_{\text{SUSY}}^2, B\mu)$ necessary for obtaining a large Higgs VEV and the phase shift, respectively.

One needs to carefully consider the evolution of the axion potential after inflation ends. There must be a transition of the value of ξ from the inflationary minimum toward today's minimum. This transition necessarily induces the transition of the minimum from π to 0 in the axion potential. If this transition occurs at a time when the enhanced axion mass is still comparable to or larger than Hubble, the misalignment angle could relax to a value very different from π . To understand this constraint, we turn to the post-inflationary evolution of the Higgs fields.

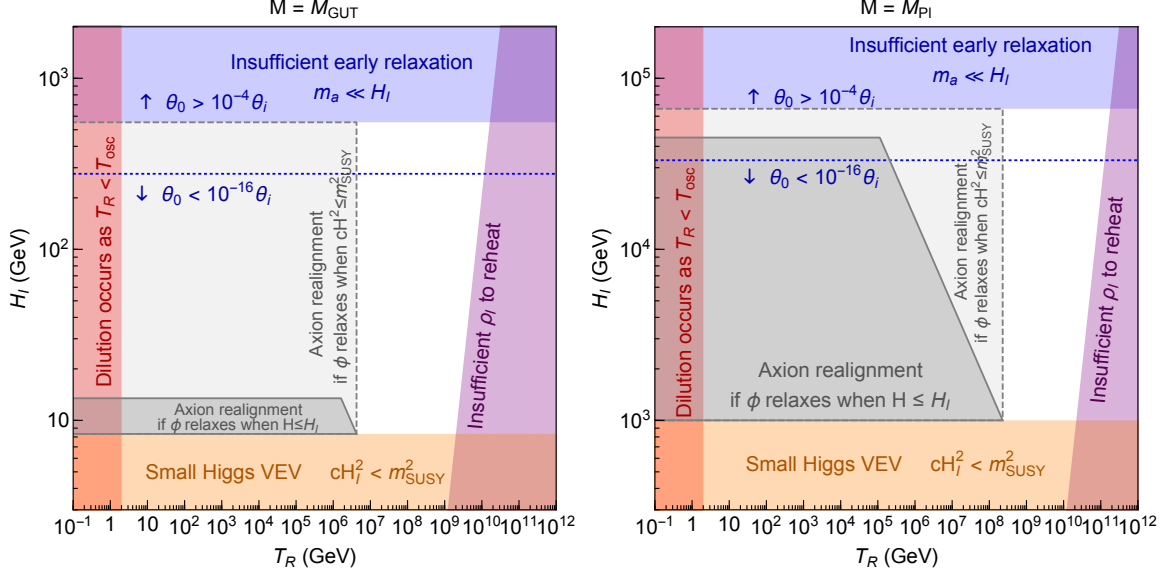


Figure 3.1: Parameter space for the inflationary Hubble scale H_I and reheat temperature T_R given $f_a = 3 \times 10^9$ GeV, $m_{\tilde{g}} = m_{\text{SUSY}} = \text{TeV}$, $B\mu = m_{\text{SUSY}}^2 / \tan\beta$, $\tan\beta = 50$, $N_e = 60$, and $\phi_i = M$. The left (right) panel is for the cutoff scale $M = M_{\text{GUT}}$ (M_{Pl}) respectively.

The Hubble induced mass terms which stabilize ϕ at a large VEV are tied to the inflaton energy density. If the sign of the Hubble induced terms remains the same after inflation, ϕ continues to be trapped around M . This means the radial and angular directions of the Higgs fields do not oscillate until the Hubble induced terms become subdominant to the MSSM soft terms of the corresponding mode as the inflaton energy density redshifts and/or decays.

A second possibility for this evolution is that the sign of the Hubble induced mass flips after inflation (except for the $H_u H_d$ term.) This may occur in two-field inflation models. For example, with $K = (-c_Z |Z|^2 + c_{\bar{Z}} |\bar{Z}|^2) |\phi|^2$ with $c_Z > c_{\bar{Z}}$ and $W = m_Z Z \bar{Z}$, we assume that the scalar component of Z acquires a large field value and drives inflation. It is \bar{Z} whose F -term, $F_{\bar{Z}}^2 = m_Z^2 \phi_Z^2$, is non-zero. During inflation, the kinetic energy of ϕ_Z is much smaller than its potential energy, i.e. $|\partial_\mu Z|^2 \ll F_{\bar{Z}}^2$, and thus the Hubble induced mass for ϕ is negative. As inflation ends, Z 's potential and kinetic energies become comparable but, since $c_Z > c_{\bar{Z}}$, the sign of the Hubble induced mass

for the Higgs radial mode flips to positive. Consequently, ϕ is no longer trapped at a large VEV but oscillates towards the origin immediately after inflation. The early onset of radial oscillations helps because a longer period of redshifting in ϕ suppresses Λ'_{QCD} , which leads to the desired post-inflationary suppression of the axion mass.

It is only necessary to track the ratio m_a/H between the onset of angular oscillations at $cH^2 = B\mu$ and thermalization of the Higgs fields. During this period, the Higgs phase ξ can evolve and with it comes the shift in the axion potential. If the axion mass is subdominant to Hubble friction, however, the axion field is overdamped and remains agnostic to this evolution. When the Higgs is finally thermalized, its energy density is depleted and the field is quickly set to the minimum today, removing the axion mass enhancement. As a result, to preserve the prediction of the axion misalignment angle, m_a/H needs to stay under unity during this period.

Thermalization of the Higgs is mediated by scattering with gluons via a loop-suppressed operator [32, 114]

$$\Gamma_h = \frac{B}{16\pi^2} \frac{T^2}{\phi}, \quad (3.12)$$

with $B \simeq 10^{-2}$ and ϕ identified as the oscillation amplitude. Interestingly, due to the scaling properties during a matter-dominated era, the Higgs scattering generates a radiation energy density that is constant in time, whose contribution to thermal bath's temperature is

$$T_h = \left(\frac{30}{\pi^2 g_*(T_h)} \frac{B}{16\pi^2} \right)^{1/2} \left(\frac{m_\phi^2 \phi_i}{H_I} \right)^{1/2}, \quad (3.13)$$

with ϕ_i as the field value of the Higgs at the end of inflation. This radiation persists throughout the evolution until the Higgs fields are thermalized at $H \simeq \Gamma_h$. This radiation is important because in some cases it can dominate over the radiation produced from the inflaton decay and cause a period of a constant temperature in the cosmological evolution. This has the effect of maintaining the finite temperature

suppression to the axion mass

$$m_a(T) = \frac{1}{4\pi} \frac{m_{\tilde{g}}^{1/2} \Lambda_{\text{fid}}^{3/2}}{f_a} \left(\frac{\Lambda'_{\text{QCD}}}{T} \right)^n, \quad (3.14)$$

where $n = 3$ ($n = 0$) for $T > \Lambda_{\text{QCD}}$ ($T < \Lambda_{\text{QCD}}$). The temperature dependence is determined by the contribution from the gauge multiplets, while the contribution from chiral multiplets vanishes because of the cancellation between the RGE contribution and the fermion mass suppression. In the extended models, Λ'_{QCD} may be different from the estimate in Eq. (3.8) because of the backreaction from strong QCD dynamics. We note that the value of m_a evolves after inflation not only due to this temperature suppression, but also its explicit dependence on $\Lambda_{\text{fid}} \propto \phi^{2/3}$, which evolves as the Higgs oscillation amplitude redshifts until the Higgs fields thermalize and settle into today's vacuum. "Including the decrease in Λ'_{QCD} from the redshift in $\phi \propto H^{\frac{1}{1+w}}$, with the equation of state of the total energy density w , the axion mass scales like $m_a|_{\text{MD}} \propto H^{\frac{3+2n}{3}}/T^n$ during the early matter-dominated era ($w = 0$) and $m_a|_{\text{RD}} \propto H^{\frac{3+2n}{4}}/T^n$ during the radiation-dominated era ($w = 1/3$) after reheating." These considerations of the Higgs oscillations and axion mass suppression are taken into account when determining the post-inflationary constraint in the regions shaded in dark gray (light gray enclosed by the dashed contour) in Fig. 3.1 assuming that the radial direction starts oscillation at $\sqrt{c}H \simeq m_{\text{SUSY}}$ (right after inflation) respectively. This constraint is milder in the left panel because $M = M_{\text{GUT}}$ starts out with a smaller axion mass during inflation than $M = M_{\text{Pl}}$ so m_a/H is more likely to be less than unity during the transition period. In fact, these gray regions disappear for $M \lesssim 10^{16}$ GeV opening up regions of low T_R even though the blue constraint becomes stronger.

Another requirement of DAMP $_{\pi}$ comes from avoiding PQ symmetry restoration. In a thermal environment, the PQ breaking field saxion P acquires a thermal mass $y^2 T^2 P^2$ because of the Yukawa coupling $y P Q \bar{Q}$ with the PQ quarks Q, \bar{Q} . This

thermal mass can be relevant at large temperatures and stabilize P at a vanishing value to restore PQ symmetry. This can be easily prevented if the symmetry breaking is enforced by the following superpotential,

$$\Delta W_P = \lambda S (P\bar{P} - f_a^2). \quad (3.15)$$

The F -term of S stabilizes P and \bar{P} in the moduli space $P\bar{P} = f_a^2$ to break PQ. The coupling constant λ may be as large as 4π in strongly coupled models [79, 82]. To ensure that PQ is not thermally restored after inflation where the maximum temperature achieved during reheating is $T_{\max} \simeq (H_I M_{\text{Pl}} T_R^2)^{1/4}$,⁴ the thermal mass must be less than $\lambda f_a < 4\pi f_a$ at this time, giving an upper bound on the Yukawa coupling

$$y \lesssim 1.5 \left(\frac{m_{P,\bar{P}}}{f_a} \right) \left(\frac{f_a}{3 \times 10^9 \text{ GeV}} \right) \left(\frac{\text{TeV}}{H_I} \right)^{1/4} \left(\frac{10^{10} \text{ GeV}}{T_R} \right)^{1/2}, \quad (3.16)$$

which can be easily satisfied with $y \lesssim \mathcal{O}(1)$ in the allowed parameter space of Fig. 3.1. The constraint is stronger if the mass of the PQ symmetry breaking field is only as large as m_{SUSY} , but we do not pursue this issue further.

A runaway potential for P is generated by strong dynamics via $W_{\text{eff}} \simeq (1/4\pi)^2 \Lambda_{\text{fid}}^3 (P/f_a)^{1/3}$, which introduces an effective saxion mass of order $(1/4\pi)^2 \Lambda_{\text{fid}}^3/f_a^2$. Keeping in mind the dependence of Λ_{fid} on both the cutoff scale M and $\tan\beta$ from Eq. (3.11), we find this effective saxion mass for the parameters in Fig. 3.1 to be of order 10^2 GeV (10^6 GeV) for $M = M_{\text{GUT}}$ (M_{Pl}) respectively. For values of H_I in the allowed parameter space, a Hubble induced mass for P is not always large enough to stabilize P . For simplicity, we stabilize P by superpotential terms $W = m_P P Y + m_{\bar{P}} \bar{P} \bar{Y}$. The F -terms of Y and \bar{Y} give large masses $m_P \sim m_{\bar{P}}$ to P and \bar{P} . These masses can be as large as $4\pi f_a$

⁴The actual maximal temperature is smaller after taking into account the efficiency of the thermalization [83].

without destroying the moduli space $P\bar{P} = f_a^2$ and are large enough to stabilize P against the runaway potential. The quarks Q and \bar{Q} have a large mass yP , which allows us to neglect the effects of their Hubble induced masses in the minimal models. We will see in Sec. 3.3.2 that larger values of Λ'_{QCD} and H_I will modify the dynamics of these fields.

Finally, the purple regions in Fig. 3.1 are excluded by energy conservation which restricts the reheat temperature T_R to a maximum value dictated by the energy in the inflaton, $\rho_I \simeq M_{\text{Pl}}^2 H_I^2 \gtrsim T_R^4$. In the red regions, the axion starts to oscillate from the hilltop towards today's minimum during a matter-dominated era by the inflaton, in which case reheating produces entropy, dilutes the axion abundance, and spoils the prediction of a small f_a . Even though the minimal model has proven to provide a viable cosmology for DAMP $_{\pi}$, we explore extended models in the following subsection to further broaden the parameter space.

3.3.2 Extended Models

The most stringent constraint in the minimal model is a relatively low upper bound on H_I due to difficulties in enhancing the axion mass during inflation. As shown in Eq. (3.11), we can enhance Λ'_{QCD} , and consequently m_a , by introducing additional matter content. As we raise the value of Λ'_{QCD} , the values of fields in the PQ sector may be shifted from the one in the vacuum and impact the evaluation of the axion mass. The field value of the Higgs may be also affected.

We consider a simple model where a PQ symmetry breaking field P couples to KSVZ quarks $Q\bar{Q}$ by a Yukawa coupling y [103, 135]. We need to reliably evaluate the VEVs of both P and $Q\bar{Q}$, as both are PQ charged and the decay constant during inflation f_I is given by the larger of P and $(Q\bar{Q})^{1/2}$. The superpotential of P and $Q\bar{Q}$ is

$$W = \frac{1}{(4\pi)^3} \frac{\tilde{\Lambda}^4}{(Q\bar{Q})^{1/2}} + yPQ\bar{Q}, \quad (3.17)$$

where the first term is the non-perturbative Affleck-Dine-Seiberg superpotential [17]. The scale $\tilde{\Lambda}$ is related with Λ_{fid} via

$$\tilde{\Lambda} = \Lambda_{\text{fid}} \left(\frac{\Lambda_{\text{fid}}}{y f_a} \right)^{1/8}. \quad (3.18)$$

The relation can be obtained by comparing the effective superpotential after integrating out $Q\bar{Q}$ from Eq. (3.17) and the effective potential

$$W_{\text{eff}} \simeq \frac{1}{(4\pi)^2} \Lambda_{\text{fid}}^3 \left(\frac{P}{f_a} \right)^{1/3}, \quad (3.19)$$

where the effect of a P field value different from f_a is included. Note that the potential of P from strong dynamics exhibits a runaway behavior, $\partial W_{\text{eff}}/\partial P \propto P^{-2/3}$. For this reason, we introduce a higher dimensional term $|P|^6/M^2$ to further stabilize P at a large field value which can come from a superpotential term $(\chi/M)P^3$, where χ is a chiral field. We also consider the Hubble induced mass of P and $Q\bar{Q}$. Explicitly we take

$$\Delta V \simeq c H_I^2 |Q|^2 + c H_I^2 |\bar{Q}|^2 - c H_I^2 |P|^2 + \frac{|P|^6}{M^2}. \quad (3.20)$$

We stress that these terms are used in our analysis but they are not the only possible extensions to DAMP_π . The sign of the Hubble induced mass of Q and \bar{Q} is taken to be positive to ensure that Q is not destabilized by the Hubble induced mass. We study a negative Hubble induced mass for P for the following reason. We find that $Q > P$ and hence f_I is dominated by Q for this choice of the signs. If the Hubble induced mass of P is positive instead, the field value of P becomes smaller and makes the field value of Q larger because of the smaller mass of Q . This increases f_I while decreasing the dynamical scale and suppressing the axion mass.

As the Hubble induced mass of Q breaks the supersymmetry of the QCD sector, the axion mass may non-trivially depends on the parameters. When yP is larger than

$Q, Q\bar{Q}$ can be integrated out at the mass threshold yP and the effective potential is given by Eq. (3.19). The axion mass is given by

$$m_a \simeq \frac{1}{4\pi} \frac{m_{\tilde{g}}^{1/2} \Lambda_{\text{fid}}^{3/2}}{f_I} \left(\frac{P}{f_a} \right)^{1/6}. \quad (3.21)$$

If Q is larger than yP , the theory below the mass threshold Q is a supersymmetric, pure $SU(2)$ gauge theory with a dynamical scale $\tilde{\Lambda}(\tilde{\Lambda}/Q)^{1/3}$. The axion mass is then given by

$$m_a \simeq \frac{1}{4\pi} \frac{m_{\tilde{g}}^{1/2} \tilde{\Lambda}^{3/2}}{f_I} \left(\frac{\tilde{\Lambda}}{4\pi Q} \right)^{1/2} = \frac{1}{4\pi} \frac{m_{\tilde{g}}^{1/2} \Lambda_{\text{fid}}^{3/2}}{f_I} \left(\frac{\Lambda_{\text{fid}}^3}{16\pi^2 y f_a Q^2} \right)^{1/4}. \quad (3.22)$$

Note that the two formulae agree with each other when the field value of Q is determined by the F -term condition of $Q\bar{Q}$ from the superpotential in Eq. (3.17).

Strong dynamics also affects the Higgs. The effective superpotential of ϕ is given by

$$W \simeq \frac{\Lambda_{\text{eff}}^3}{16\pi^2} \left(\frac{\phi}{M} \right)^2, \quad \Lambda_{\text{eff}}^3 = \begin{cases} \Lambda_{\text{fid}}^3 \left(\frac{P}{f_a} \right)^{1/3} & yP > Q \\ \Lambda_{\text{fid}}^3 \left(\frac{\Lambda_{\text{fid}}^3}{16\pi^2 y f_a Q^2} \right)^{1/2} & yP < Q. \end{cases} \quad (3.23)$$

This gives the Higgs a mass $\simeq \Lambda_{\text{eff}}^3/(16\pi^2 M^2)$, which should be smaller than $\sqrt{c}H_I$.

By computing and comparing the axion mass to H_I , we put an upper bound on the allowed values of H_I such that DAMP_π 's first criterion is fulfilled during inflation, which is shown in Fig. 4.1. In deriving the blue-shaded region, we integrate out $Q\bar{Q}$, obtain the scalar potential of P from the effective potential Eq. (3.19), add the potential of P in Eq. (3.20), determine the field value of P during inflation, and compute the axion mass. This corresponds to the case where Q is actually determined by the F -term condition $\partial W/\partial Q = 0$. The gray contours show the constraint using the full potential described above. As y becomes larger the constraints approach to the

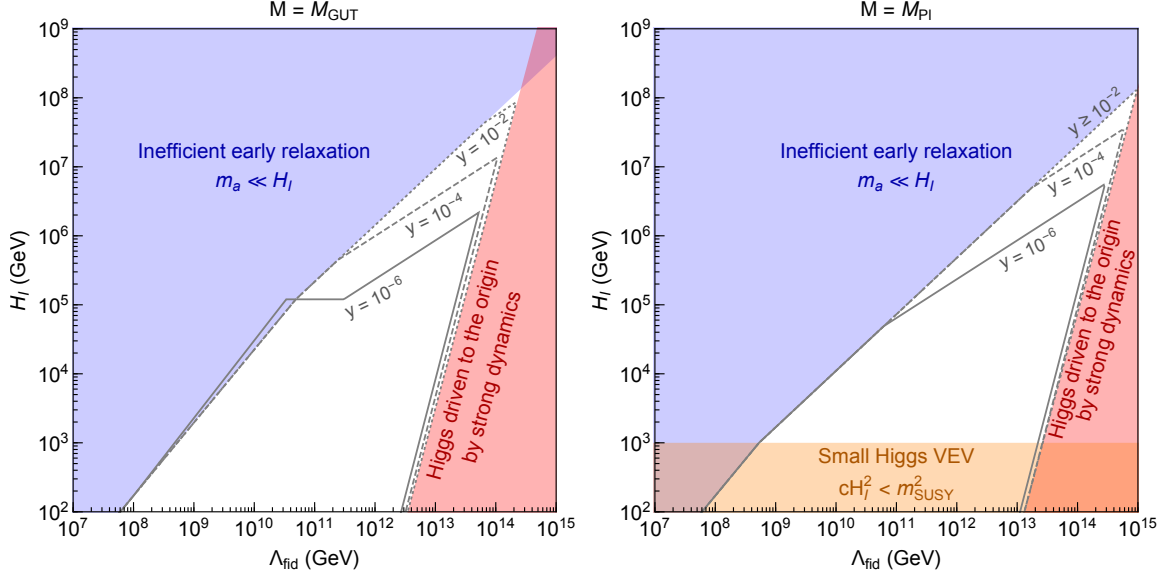


Figure 3.2: Parameter space for the inflationary Hubble scale H_I and the fiducial confinement scale Λ_{fid} defined in Eq. (3.8) given $f_a = 3 \times 10^9$ GeV, $m_{\tilde{g}} = m_{\text{SUSY}} = \text{TeV}$, and $\phi_i = M$. The left (right) panel is for the cutoff scale $M = M_{\text{GUT}}$ (M_{Pl}) respectively.

blue-shaded region. An additional constraint shown in the red regions arises because strong dynamics drives the Higgs to the origin.

In computing the field values of P and Q , we treat Q as a canonically normalized field. This is a good approximation if yP or Q is above the dynamical scale. We find that in the allowed parameter space, either yP or Q is no smaller than one order of magnitude below the dynamical scale so we expect the approximation gives a good order of magnitude estimate.

We now discuss the post-inflationary evolution and constraints similar to Sec. 3.3.1. Although this study is comprehensive in evaluating the inflationary constraints, the thermal masses for P and Q dramatically complicate PQ dynamics during and after reheating. Nonetheless, we are able to identify a large allowed parameter space in the H_I, T_R plane in the following way. There exists a wide region where the Higgs fields thermalize before the Higgs angular mode ξ begins to oscillate so that Λ'_{QCD} is quickly set to today's value Λ_{QCD} before ξ has a chance to evolve and shift the

axion potential. Physically, this means that the axion potential turns off before the location of its minimum shifts. Therefore, the prediction of the misalignment angle is automatically preserved without the need to track the post-inflationary evolution of P and $Q\bar{Q}$. This is the case when the Higgs scattering rate in Eq. (3.12) equals the Hubble rate before cH^2 drops below $B\mu$. This region is described by an allowed window of T_R for a given H_I

$$T_R \gtrsim 10^8 \text{ GeV} \left(\frac{M}{M_{\text{GUT}}} \right)^{3/2} \left(\frac{B\mu}{\text{TeV}} \right)^{3/4} \left(\frac{\phi_i}{M_{\text{GUT}}} \right) \left(\frac{10^5 \text{ GeV}}{H_I} \right), \quad (3.24)$$

$$T_R \lesssim 6 \times 10^{11} \text{ GeV} \left(\frac{M_{\text{GUT}}}{M} \right)^{3/2} \left(\frac{\text{TeV}}{B\mu} \right)^{3/4} \left(\frac{H_I}{10^5 \text{ GeV}} \right)^2 \left(\frac{M_{\text{GUT}}}{\phi_i} \right)^2, \quad (3.25)$$

where the two distinct formulae come from thermalization during the matter- and radiation-dominated epochs respectively. This window becomes wider as H_I increases so as long as

$$H_I > 6 \text{ TeV} \left(\frac{M}{M_{\text{GUT}}} \right) \left(\frac{B\mu}{\text{TeV}} \right)^{1/2} \left(\frac{\phi_i}{M_{\text{GUT}}} \right) \quad (3.26)$$

a consistent range of T_R exists. The upper bound on H_I ultimately enters from the inflationary constraint shown in the blue regions of Fig. 4.1.

We now comment on one plausible extension to further open up the parameter space with higher H_I . The gluino mass affects the axion mass as in Eq. (3.9) and is assumed to stay invariant between inflation and today. If $m_{\tilde{g}}$ is also larger during inflation, the axion mass and the upper bound on H_I can be raised by as much as $(\Lambda_{\text{fid}}/m_{\tilde{g}})^{1/2}$, making high scale inflation easily compatible with DAMP $_{\pi}$.

With respect to PQ restoration in the extended models, we can assume the same PQ breaking mechanism as in Sec. 3.3.1 so the constraint in Eq. (3.16) applies equally here.

While the post-inflationary constraints are not fully evaluated, these extended models have been shown capable of fulfilling the criteria of DAMP $_{\pi}$ while extending the allowed parameter space to much higher H_I than in Sec. 3.3.1.

CHAPTER IV

Axions Dynamically Driven to the Origin

In this paper, we investigate a mechanism we dub Dynamical Axion Misalignment Production (DAMP), which exhibits the following two features 1) the axion field dynamically relaxes to the minimum of the potential in the early universe and 2) the model possesses a non-trivial prediction between the minima of the axion potential in the early and today's epochs. If the minima are approximately aligned, a small misalignment angle can dynamically arise without any fine-tuning, a scenario we refer to as DAMP₀. This damping effect automatically occurs when the assumption of $m_a \ll H_I$ is relaxed because the axion starts to oscillate during inflation and the amplitude is exponentially redshifted. We consider the case where the large axion mass originates from a large QCD scale during inflation. Such a scenario has been considered in Refs. [60, 27, 46], but not all constraints, such as the effects from a large QCD scale on Higgs and other scalars, are fully evaluated. Hence, the examples presented in these studies may or may not be fully compatible with cosmological bounds.

As a proof of principle, we demonstrate that DAMP₀ can be realized in an extended Minimal Supersymmetric Standard Model (MSSM). The axion mass increases with the QCD confinement scale Λ_{QCD} . By virtue of a negative Hubble induced mass via the coupling with the inflaton, the Higgs can be driven towards a large field value

along the D -flat direction. The quark masses enhanced by a large Higgs vacuum expectation value (VEV) in turn cause strong dynamics to confine at a higher scale Λ'_{QCD} via the renormalization group (RG) running, thereby enhancing m_a . If only MSSM quark masses are raised, the resultant dynamical scale is not large enough to fulfill the first criterion of DAMP₀, which urges us to consider an extended MSSM. Earlier studies in Refs. [60, 27] use generic moduli fields to directly raise the QCD scale in an attempt to achieve DAMP₀ but do not carefully examine if the axion mass can be raised in a consistent way. Ref. [46] investigates the consistency and concludes that the axion mass cannot be raised above the Hubble scale during inflation. We will clarify why our setup evades their claim. Later studies in Refs. [91, 45] introduce an extra $SU(3)_c$ charged particle and raise their masses by the large Higgs VEV. The purpose of the papers is to suppress the isocurvature perturbations and no attempts are made in fulfilling the second criterion for DAMP₀ to make predictions about the DM abundance.

The second criteria of DAMP₀ can be satisfied by an (approximate) CP symmetry of the theory ensuring that the minimum of the axion potential is nearly the same during inflation and in the vacuum [27]. For example, the field values of any moduli which change the QCD θ term should remain unchanged. This can be understood by a CP symmetry which differentiates CP-odd moduli from CP-even moduli, and by assuming that the CP-odd moduli are always fixed at the enhanced symmetry points. Also, in the extended MSSM we introduce extra $SU(3)_c$ charged particles whose masses are large during inflation. The phase of the masses should be nearly aligned with that in the vacuum, which can be ensured by an approximate CP symmetry. We must introduce $\mathcal{O}(1)$ CP violation in the Yukawa couplings of the MSSM. We assume that the coupling among the source of CP violation, the moduli fields, and the extended sector is small, which may be understood by some symmetry or a geometrical separation in extra dimensions. Even if the CP phase is $\mathcal{O}(1)$ in the Yukawa couplings, perturbative

quantum corrections to the moduli and the extended sectors are expected to be small, as the CP phase of the Yukawa couplings is physical only if three generations are simultaneously involved, suppressing the possible quantum corrections by multi-loop factors, the small Yukawa couplings, and generation mixings.¹

A truly vanishing misalignment angle will imply the absence or a different origin of axion dark matter. Both of these are interesting possibilities, especially if DAMP₀ is applied to the fine-tuning problem in string axions. In this paper, we focus on QCD axion dark matter from the misalignment mechanism with $M_{\text{GUT}} \lesssim f_a \lesssim M_{\text{Pl}}$, and thus a finite $10^{-4} \lesssim \theta_{\text{mis}} \lesssim 10^{-3}$ is necessary. This implies that axion’s minimum during inflation should nearly but not precisely coincide with today’s value. One possibility is that the desirable amount of the CP-violating phase exists. Another possibility is with $H_I \simeq m_a$ so that inflation ends exactly at the time when θ_{mis} is relaxed to the desired value. We limit our consideration to the former and assume an approximate CP symmetry in the Higgs, inflaton, and extended sectors.² Interestingly, the CP violation in the MSSM around the TeV scale is currently constrained to $\mathcal{O}(10^{-3})$ by the electron dipole moment [20, 44] and might be detected in future experiments if CP violation of $\mathcal{O}(10^{-4}\text{--}10^{-3})$ exists in the Higgs sector.

In Sec. 4.1, we review the misalignment mechanism for axion dark matter. In Sec. 4.2, we illustrate in detail how the understanding of the misalignment angle can be dramatically different when the dynamics of the Higgs during inflation is taken into account. We summarize and discuss the conditions and implications of DAMP₀.

¹One may wonder that solving the strong CP problem by the CP symmetry without resorting to the QCD axion is more minimal. In fact, it is not easy to solve the strong CP problem while generating $\mathcal{O}(1)$ complex phases in the Yukawa couplings, as the complex phases readily correct the θ term. See Refs. [116, 28, 31, 85] for models which work under several assumptions.

²Suppressing the CP-violating phase is not sufficient in ensuring $\theta_{\text{mis}} \ll 1$ because the parameters setting the axion minimum can be real but change signs during and after inflation, introducing a phase shift of $\arg(-1) = \pi$ in the potential. Equivalently, the axion minimum is converted to the hilltop, i.e. $\theta_{\text{mis}} \simeq \pi$. We explore this possibility called DAMP _{π} in a separate publication [50].

4.1 Misalignment Mechanism

Since DAMP₀ operates at times well before the weak scale, it simply sets the initial condition for the standard misalignment mechanism [127, 2, 56], which we will review in this section. When the temperature drops to near the QCD scale, the axion acquires a periodic potential energy through the color anomalies, with a mass given by

$$m_a(T \geq \Lambda_{\text{QCD}}) = 6 \text{ eV} \left(\frac{10^6 \text{ GeV}}{f_a} \right) \left(\frac{\Lambda_{\text{QCD}}}{T} \right)^n, \quad (4.1)$$

where $n = 4$ for the SM is obtained by the dilute instanton gas approximation (see the lattice simulations in Refs. [125, 34, 40, 33, 73], whose results indicate that n ranges from 3.0 to 3.7 depending on the temperature). The equation of motion and the energy density read

$$\ddot{\theta}_a + 3H\dot{\theta}_a = -m_a^2\theta_a, \quad (4.2)$$

$$\rho_a = \frac{1}{2} (m_a^2 \varphi^2 + \dot{\varphi}^2), \quad (4.3)$$

where the axion field value φ is interchangeable with the angle $\theta_a \equiv \varphi/f_a$. Initially overdamped by the Hubble friction term in Eq. (4.2), the axion mass increases through the QCD phase transition and the axion starts to oscillate coherently when $m_a \simeq 3H$. After the onset of oscillations, the axion behaves as cold dark matter with the abundance given in Eq. (??). Assuming the axion reproduces the observed DM abundance, a small θ_{mis} leads to the prediction of large f_a

$$f_a \simeq 2 \times 10^{16} \text{ GeV} \left(\frac{2 \times 10^{-3}}{\theta_{\text{mis}}} \right)^{\frac{2n+4}{n+3}}, \quad (4.4)$$

where $n = 0$ is understood for $f_a \gtrsim 10^{17} \text{ GeV}$ as the axion mass reaches the zero-temperature value before the oscillation starts. In what follows, we illustrate on how

a small θ_{mis} can naturally arise from dynamics via DAMP₀, as opposed to fine-tuning the initial condition.

4.2 Early Relaxation during Inflation

The axion field is generically assumed to be a constant during inflation as a result of the Hubble friction term in Eq. (4.2) because one presumes that the axion mass is no larger than today's value. Nonetheless, this assumption holds only when the effects responsible for the axion mass remain invariant throughout the cosmological evolution. If the axion mass is larger than the Hubble parameter during inflation H_I , the axion begins its coherent oscillations, whose amplitude is damped exponentially. The axion mass may initially be enhanced by a smaller decay constant, a larger QCD scale, or a different origin of the axion mass. A smaller decay constant can occur when the PQ breaking dynamics evolves with time, whereas the axion may also receive extra mass contributions, e.g. a large QCD confinement scale [60, 27, 46, 91, 45, 89], explicit PQ breaking [84, 100, 141, 101], and magnetic monopoles [99, 118].

We study the scenario where the QCD scale is enhanced by the inflationary dynamics of the Higgs or other moduli fields. QCD confines at the scale where strong dynamics becomes non-perturbative from the RG running. The number of active quark flavors affects the RG running and, in particular, Λ_{QCD} increases with the quark masses. Consequently, the quark masses that are raised during inflation, e.g. by the Higgs VEV, increase the QCD scale and hence the axion mass. Other generic moduli fields can also directly affect the gauge coupling constant [60, 27, 46, 89] and thus the QCD scale as well. We first discuss the minimal setup of the MSSM and a large Higgs VEV before introducing additional particles.

The Higgs evolution during inflation crucially depends on its coupling with other fields. If a negative mass term is generated by the VEVs of other scalars and dominates over the Hubble scale, the Higgs field is driven to a large value where higher dimensional

operators become important in stabilizing the Higgs. The MSSM provides a well-motivated framework for this realization. To be concrete, we assume the following Kähler potential

$$\Delta K = \frac{|X|^2}{M^2} \left(|H_u|^2 + |H_d|^2 + (H_u H_d + c.c.) - \frac{|H_u|^2 |H_d|^2}{M^2} - \frac{|H_u|^4}{M^2} - \frac{|H_d|^4}{M^2} \right), \quad (4.5)$$

where X is the chiral field whose F -term provides an inflaton energy and M is the cutoff scale of the theory. Here and hereafter we assume a universal cutoff and drop $\mathcal{O}(1)$ coefficients. Through Eq. (4.5), the energy density of the inflaton $\rho_X = F_X F_X^* \simeq H_I^2 M_{\text{Pl}}^2$ generates the Hubble induced mass as well as the higher dimensional operators in the Higgs potential

$$\Delta V = c H_I^2 \left(-|H_u|^2 - |H_d|^2 - (H_u H_d + c.c.) + \frac{|H_u|^2 |H_d|^2}{M^2} + \frac{|H_u|^4}{M^2} + \frac{|H_d|^4}{M^2} \right), \quad (4.6)$$

where $c = M_{\text{Pl}}^2/M^2$. These additional Hubble induced terms in Eq. (4.6) affect both the radial and angular directions of the Higgs fields. The negative Hubble induced mass, $-c H_I^2 (|H_u|^2 + |H_d|^2)$, drives the Higgs along the D -flat direction $|H_u| = |H_d| \equiv \phi$ towards large VEVs of order M , which are stabilized by the positive quartic terms. This enhances the axion mass via a larger dynamical scale from heavier quarks. We note that the Higgs energy density is comparable to that of the inflaton and makes an $\mathcal{O}(1)$ change to the vacuum energy. Since the Higgs field value remains constant and the Higgs energy density follows that of the inflaton, this only changes the overall energy scale of the inflation and does not interfere with inflation dynamics. Conversely, if the sign of $c H_I^2 (|H_u|^2 + |H_d|^2)$ is positive instead, the conventional cosmology results because the Higgs VEVs remain small. Finally, the term $-c H_I^2 (H_u H_d + c.c.)$ fixes the relative phase of H_u and H_d .³ This term is not necessary if the vacuum $B\mu$ term is

³Ref. [46] does not introduce this term and relies on the vacuum $B\mu$ term to fix the phase.

already larger than H_I^2 . We assume an approximate CP symmetry so that this Higgs phase is nearly aligned with today's value,⁴ satisfying the second criterion of DAMP₀. Here $\sqrt{c}H_I$ is assumed to be larger than the supersymmetry (SUSY) soft breaking scale m_{SUSY} and hence we need

$$H_I \gtrsim 10 \text{ GeV} \left(\frac{m_{\text{SUSY}}}{\text{TeV}} \right) \left(\frac{M}{M_{\text{GUT}}} \right), \quad (4.7)$$

where $M_{\text{GUT}} = 2 \times 10^{16} \text{ GeV}$. We may relax this condition if the μ term as well as the soft SUSY breaking terms are small at large field values of the Higgs or during inflation. The soft terms are actually smaller in gauge mediation since the large Higgs field value breaks the gauge symmetry.

The large Higgs VEV gives quarks very large masses during inflation. In the MSSM, the 1-loop renormalization group equation (RGE) is

$$\mu_r \frac{d}{d\mu_r} \frac{8\pi^2}{g^2} = 3N - F, \quad (4.8)$$

where μ_r is the renormalization scale, N is the gauge group index, and F is the number of active fermions in the theory. In the MSSM with a large Higgs VEV ϕ_i , assuming the gauge couplings are held fixed at the GUT scale, and pretending that all quarks (including possible KSVZ quarks [103, 135]) are heavier than the dynamical scale, we find that the fiducial dynamical scale is raised to

$$\Lambda_{\text{fid}} = 10^7 \text{ GeV} \left(\frac{\phi_i}{10^{16} \text{ GeV}} \right)^{2/3} \left(\frac{\tan\beta}{1} \right)^{1/3}. \quad (4.9)$$

They hence restrict their attention to the case where $H_I < m_{\text{SUSY}}$. Furthermore, they assume that $M \sim M_{\text{P1}}$, and thus the Higgs does not take a large field value during inflation. The axion mass is suppressed in their setup and DAMP₀ cannot be realized.

⁴We assume the sign of $cH_I^2(H_u H_d + c.c.)$, if required to fix the relative phase, is the same as $B\mu(H_u H_d + c.c.)$ from soft supersymmetry breaking in the present universe. Rather, if the signs are opposite, the Higgs phase shifts by π , placing the axion at the hilltop instead. We consider this interesting possibility in Ref. [50].

The fiducial dynamical scale coincides with the physical dynamical scale Λ'_{QCD} if all quarks are actually heavier than Λ_{fid} . Otherwise, they are related as

$$\Lambda_{\text{fid}} \equiv \Lambda'_{\text{QCD}} \prod_{m_q < \Lambda'_{\text{QCD}}} \left(\frac{m_q}{\Lambda'_{\text{QCD}}} \right)^{1/9}. \quad (4.10)$$

When the physical dynamical scale is raised beyond the gluino mass $m_{\tilde{g}}$, the axion mass is suppressed by $m_{\tilde{g}}$ as

$$m_a \simeq \frac{1}{4\pi} \frac{m_{\tilde{g}}^{1/2} \Lambda_{\text{fid}}^{3/2}}{f_a} \simeq 10 \text{ keV} \left(\frac{m_{\tilde{g}}}{\text{TeV}} \right)^{1/2} \left(\frac{\Lambda_{\text{fid}}}{10^7 \text{ GeV}} \right)^{3/2} \left(\frac{10^{16} \text{ GeV}}{f_a} \right), \quad (4.11)$$

where we include the factor of 4π expected from the naive dimensional analysis [110, 69, 108, 52]. The mass $m_{\tilde{g}}$ refers to the RG invariant quantity, $m_{\tilde{g},\text{phys}}/g^2$. This suppression can be understood by the R symmetry in the limit of a vanishing gluino mass, where only a linear combination of an R -axion and the QCD axion, which is dominantly the R axion, obtains a mass from the color anomaly. The axion mass is given by Λ_{fid} rather than the physical dynamical scale. This can be understood by computing the axion mass in the parameter space where $\Lambda_{\text{fid}} = \Lambda'_{\text{QCD}}$, and extending it to the case with $\Lambda_{\text{fid}} < \Lambda'_{\text{QCD}}$ by holomorphy of the gauge coupling. The MSSM with a large Higgs VEV alone is insufficient in raising the axion mass above the scale of H_I required in Eq. (4.7) to drive the Higgs towards the D -flat direction. Even if we avoid the bound in Eq. (4.7) by small m_{SUSY} in the early universe, the Hubble scale during inflation must be below the MeV scale, which may require fine-tuning in the inflation model parameters.

One can further enhance Λ_{fid} by introducing additional particles. One possibility involves a moduli field whose VEV controls and increases the gauge coupling constant [60, 27, 46, 89] during inflation. To satisfy the second criterion of DAMP₀, the coupling between the moduli field and $G\tilde{G}$ should be suppressed. The field value of the CP-odd

part of the moduli field should remain the same during inflation and in the vacuum.

Another possibility is to extend the MSSM by N_Ψ additional fermion pairs in the $\mathbf{5} + \bar{\mathbf{5}}$ representation of $SU(5)$ as discussed in Ref. [91]

$$\Lambda_{\text{fid}} \simeq 10^7 \text{ GeV} \left(\frac{\phi_i}{10^{16} \text{ GeV}} \right)^{2/3} \left(\frac{M_{\Psi,I}}{M_\Psi} \right)^{N_\Psi/9}, \quad (4.12)$$

where M_Ψ and $M_{\Psi,I}$ are the vacuum mass and the enhanced mass during inflation, respectively. We can enhance the mass of Ψ by the large VEVs of some fields, which can be identified with the moduli field discussed above. The minimal example is a coupling with the Higgs, $W \sim H_u H_d \Psi \bar{\Psi} / M$. For instance, with $N_\Psi = 4$, $M_\Psi = m_{\tilde{g}} = \text{TeV}$, $M_{\Psi,I} = \phi_i = M_{\text{GUT}}$, the dynamical scale is $\Lambda_{\text{fid}} \simeq 10^{13} \text{ GeV}$; the axion mass $m_a \simeq 10^4 \text{ GeV} (10^{16} \text{ GeV} / f_a)$ sets an upper bound on H_I since efficient early relaxation to the minimum demands $m_a > H_I$. This is now consistent with Eq. (4.7). To satisfy the second requirement of DAMP₀, CP-violating phases of M_Ψ and $M_{\Psi,I}$ should be absent.

Even if the dynamical scale is raised by the dynamics of fields other than the Higgs, the large Higgs field value during inflation is still crucial. If the Higgs field value is small, the axion mass is suppressed by the small MSSM quark masses as shown in Ref. [46].

We stress that the results of DAMP₀ are independent of the specific mechanism that raises the QCD scale during inflation. Nonetheless, there are some consistency conditions to be satisfied. The suppression by light quark masses in Eq. (4.10) implies that, even when both Λ'_{QCD} and ϕ_i are saturated to the cutoff scale M , the Standard Model quark Yukawa couplings y_q set an absolute maximum of Λ_{fid}

$$\Lambda_{\text{fid}}^{\text{max}} = M \prod_{q \in \text{SM}} y_q^{1/9} \simeq 10^{-2} M. \quad (4.13)$$

Moreover, strong dynamics generates the following effective superpotential for the

Higgs,

$$W \simeq \frac{1}{16\pi^2} \left(\Lambda_{\text{fid}}|_{\phi_i=M} \right)^3 \left(\frac{\phi}{M} \right)^2 \quad (4.14)$$

and gives a mass to ϕ from the F -term potential

$$m_\phi \simeq \frac{\left(\Lambda_{\text{fid}}|_{\phi_i=M} \right)^3}{16\pi^2 M^2}, \quad (4.15)$$

which can dominate and prevent the Higgs from acquiring a large VEV. We require that this should be smaller than $\sqrt{c}H_I$. Similarly, the scalar superpartner of the axion, the saxion, also receives a mass $m_s \simeq \Lambda_{\text{fid}}^3/(f_a^2 16\pi^2)$. If the saxion mass other than this contribution is also only as large as $\sqrt{c}H_I$, we obtain a stronger constraint when $f_a < M$. The constraint is however absent if the saxion is more strongly stabilized.

The constraint on the inflationary Hubble scale H_I for a given fiducial dynamical scale Λ_{fid} is shown in Fig. 4.1. The blue region reflects the conventional cosmology without DAMP_0 for various values of f_a because the axion mass during inflation is less than H_I and the axion field is overdamped by Hubble friction. The gray region is theoretically inaccessible since Λ_{fid} exceeds the maximum in Eq. (4.13). The red region also cannot achieve DAMP_0 because strong dynamics generates a Higgs mass in Eq. (4.15) that dominates the Hubble induced mass and drives the Higgs toward the origin. In the orange region, the Hubble induced mass is subdominant to the SUSY scale in the MSSM and becomes irrelevant for $m_{\text{SUSY}} = \text{TeV}$, precluding DAMP_0 . Lastly, below the dashed line for each labeled value of f_a , the saxion mass given by strong dynamics exceeds $\sqrt{c}H_I$, and extra stabilization of the saxion is needed. For example, for a chiral multiplet S which non-linearly realizes the PQ symmetry by $S \rightarrow S + iC$, we may add a superpotential [82]

$$W = m_S f_a Z e^{-S/f_a} + m_S f_a \bar{Z} e^{S/f_a}, \quad (4.16)$$

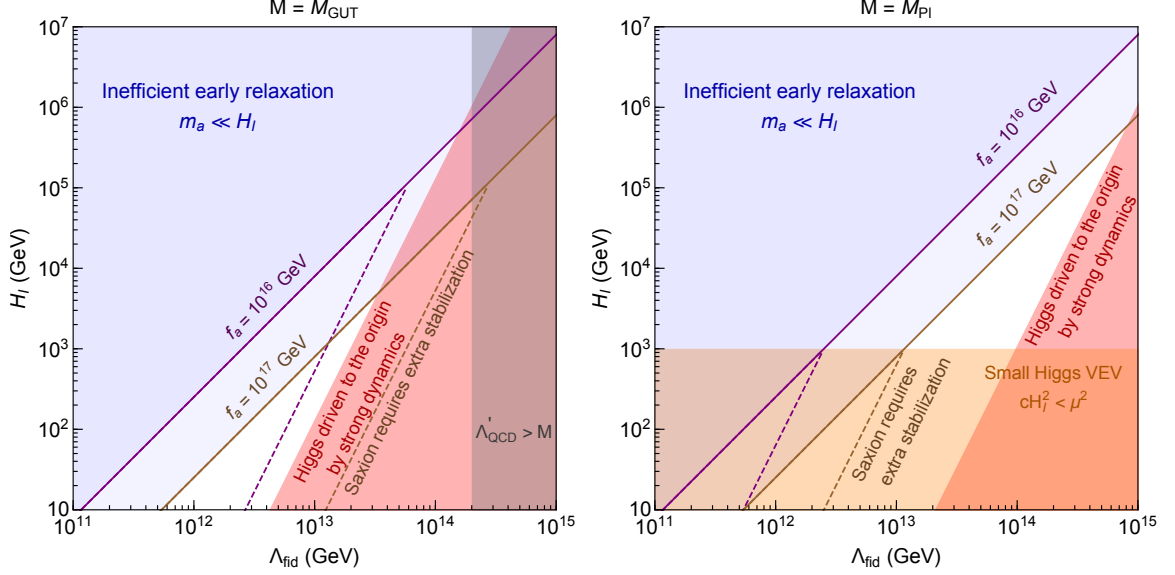


Figure 4.1: Parameter space for the inflationary Hubble scale H_I and the fiducial confinement scale Λ_{fid} defined in Eq. (4.10) given $m_{\tilde{g}} = m_{\text{SUSY}} = \text{TeV}$, and $\phi_i = M$. The left (right) panel is for the cutoff scale $M = M_{\text{GUT}}$ (M_{Pl}) respectively.

where Z and \bar{Z} are PQ charged chiral fields. This gives the saxion a mass as large as m_S . Since the F terms of Z and \bar{Z} break the supersymmetry, the mass is bounded from above,

$$m_S \lesssim m_{3/2} \frac{M_{\text{Pl}}}{f_a} \simeq 10^6 \text{ GeV} \frac{10^{16} \text{ GeV}}{f_a} \frac{m_{3/2}}{10^4 \text{ GeV}}, \quad (4.17)$$

where $m_{3/2}$ is the gravitino mass. The mass can be large enough for a realistic range of the gravitino mass.

In Fig. 4.1, we assume for minimality that the gluino mass during inflation is the same as the vacuum value that we take as $m_{\tilde{g}} = \text{TeV}$. This assumption can be relaxed as well to raise the axion mass further and broaden the allowed parameter space. If $m_{\tilde{g}}$ is larger during inflation, the upper bound on H_I can be raised by a factor as large as $(\Lambda_{\text{fid}}/m_{\tilde{g}})^{1/2} = 10^5 (\Lambda_{\text{fid}}/10^{13} \text{ GeV})^{1/2} (\text{TeV}/m_{\tilde{g}})^{1/2}$ according to Eq. (4.11). This factor is significant and DAMP_0 becomes compatible with high scale inflation.

CHAPTER V

Conclusion

5.1 Yukawa Couplings

In Chapter II, we use the geometric gauge breaking mechanism in M theory compactified on singular G_2 manifold to help understand quark and charged lepton masses. We start with the adjoint representation of a single E_8 that contains exactly three related families of quarks and leptons. Then, we break E_8 to the Standard Model via deformations and geometric engineering, following the technique of Katz and Morrison [97]. We explicitly computed Yukawa couplings in a local model and shows their fitting with experimental results.

With this approach, we hope to understand the origin of flavors and three families, and the values of quark and lepton masses. We are partially successful. We can see three families and the hierarchy of quark and lepton masses emerge. We can see the isospin breaking that makes the $SU(2)$ doublets such as top and bottom, up and down, electron and electron neutrino which all have different masses and the hierarchy of family masses. The amounts are controlled by deformation parameters that are effectively moduli. We can calculate the values of the deformation moduli that lead to the hierarchy and realistic values for the masses. Ideally, we would be able to predict the values at which the deformation moduli are stabilized, and predict the masses, but we are not yet able to do so. In principal, the moduli have to satisfy stabilization

constraints, neutrino sector, global G_2 structure, and so on. So, future study on these constraints applying to our quark and lepton context may make the theory predictive.

We are able to get some important mass values. We work with high scale Yukawa couplings. The top quark has a Yukawa coupling of order one. The up quark can be less than the down quark. More precisely, $m_{up} + m_e \lesssim m_{down}$ (ignoring an electromagnetic contribution), so that protons will be stable rather than neutrons, allowing hydrogen atoms. We can derive the conditions in the underlying theory for this inequality, or for the top Yukawa to be of order unity, but we cannot yet show they must uniquely hold. Three families and a hierarchy of masses do arise generically. The theory might not have allowed these results, so we view obtaining them in a UV complete theory as significant progress. We don't at this stage have much control over what masses are associated with the three extra $U(1)$'s, but none should be massless. Then the spectrum should contain four new Z' states. They are well motivated. In future work it may be possible to constrain their masses. Lastly, we also leave the study of the remaining particles resulted from E_8 breaking for future study.

5.2 Dynamical Axion Misalignment Production

In Chapter III and Chapter IV we discuss the fact that the misalignment mechanism can source axion dark matter in the early universe with a decay constant $f_a \simeq \mathcal{O}(10^{12})$ GeV. For $f_a \ll 10^{12}$ GeV as is of interest to many experimental searches, the observed DM abundance can be obtained if the misalignment angle θ_{mis} is taken sufficiently close to π , where the anharmonic effect becomes important. In particular, when the axion is very close to the hilltop of the potential, the onset of oscillations is delayed so the axion abundance is less redshifted and thus more enhanced. As demonstrated in Eq. (1.22), $f_a \simeq 10^{10}$ GeV corresponds to $\delta\theta \equiv \pi - \theta_{\text{mis}} \simeq \mathcal{O}(10^{-3})$, while $f_a \simeq 4 \times 10^9$ GeV already requires $\delta\theta \simeq \mathcal{O}(10^{-9})$. Such a small $\delta\theta$ has generically been understood as fine-tuning of the initial condition. In this paper, we offer an explanation to this

small $\delta\theta$ using axion dynamics in the early universe.

We point out that a class of models violates the canonical assumption that the axion field is overdamped by Hubble friction and takes a random value during inflation. Instead, there exist numerous possibilities wherein the axion is large compared to Hubble during inflation and thus relaxes to the minimum of the potential. We refer to this mechanism as Dynamical Axion Misalignment Production (DAMP). Additionally, if the model possesses an approximate CP symmetry, then the axion potential may receive a phase shift of π because the nearly real parameters for setting the axion minimum can flip the sign between inflation and the QCD phase transition. This shift converts the potential minimum into a maximum and explains why the axion is very close to the hilltop—a mechanism we dub DAMP_π .

We explicitly construct models for DAMP_π , where the higher dimensional coupling between the Higgs in the MSSM and the inflaton gives rise to a large axion mass and the phase shift of the axion potential. Specifically, a negative Hubble induced mass drives the Higgs to a large field value that enhances the quark masses, which in turn raise the QCD scale. The axion is larger than usual due to stronger QCD dynamics. Lastly, a Hubble induced $B\mu$ term that carries an opposite sign from that of the MSSM necessarily induces a shift in the axion potential by π . Together, renormalization from the SM Yukawa couplings and any additional CP violating phases in the model can provide the desired finite phase shift between $\mathcal{O}(10^{-16}\text{--}10^{-3})$. This example works only if the number of generations is odd.

Strikingly, due to the anharmonic effects of the axion potential, the prediction of f_a from the DM abundance has an extraordinarily mild logarithmic dependence on $\delta\theta \ll 1$. Therefore, DAMP_π makes a rather sharp prediction of $3 \times 10^9 \text{ GeV} \lesssim f_a \lesssim 10^{10} \text{ GeV}$. Other phenomenological features of DAMP_π are as follows. Due to early relaxation, the fluctuation of the axion field is exponentially damped and hence dark matter isocurvature perturbations are suppressed. The upper bound on H_I from isocurvature

perturbations does not apply.

The impact of this anharmonicity on the structure formation has been investigated in the literature. Refs. [144, 137] study this numerically and show that isocurvature perturbation modes whose wavelengths are larger than the horizon size are enhanced by anharmonic effects. Refs. [106, 105] numerically study the anharmonicity effects on the growth of structures arising from the large fluctuations in an inhomogeneous background, i.e. in the context of post-inflationary PQ symmetry breaking. Finally, Ref. [76] has shown that in a quasi-homogeneous region, parametric resonance can be important for amplifying fluctuations, and this effect is monotonically enhanced for larger misalignment angles. While the anharmonicity effect may stimulate structure formation, the aforementioned works are not directly applicable to this model as the isocurvature perturbations are suppressed and the PQ symmetry is already broken during inflation.

The axions from the misalignment mechanism are necessarily cold—a feature to distinguish from other non-thermal production mechanisms. It is also potentially interesting to study the imprints of maximal CP violation on the QCD phase transition as well as Big Bang nucleosynthesis.

Similarly, a large decay constant is not only within the reach of the projected experimental sensitivity for ultralight axions but well-motivated from the theoretical standpoints. Specifically, $f_a \simeq 10^{16}$ GeV can be associated with grand unification, whereas string theory predicts $f_a \simeq 10^{16-17}$ GeV. The QCD axion with such a large f_a faces serious challenges in cosmology, including overproduction of axion dark matter from the misalignment mechanism. It is widely regarded that the misalignment angle θ_{mis} can be fine-tuned to avoid this issue. Even in this case, however, isocurvature perturbations are in conflict with high scale inflation.

In this dissertation, we have identified a class of models where the misalignment angle is set to a small value due to axion dynamics instead of mere fine-tuning. The

conventional assumption of the axion field during inflation is such that Hubble friction dominates over the axion mass and the field value remains constant. Nevertheless, there are various scenarios where the axion mass can be much larger so that the axion is relaxed to the minimum in the early universe. We refer to such damping mechanism as Dynamical Axion Misalignment Production (DAMP). Furthermore, if the model possesses an approximate CP symmetry, the minima in the early universe can nearly align with that of today, leading to $\theta_{\text{mis}} \simeq 0$, which we call DAMP₀. This early relaxation to a minimum close to today's value resolves both the axion overproduction and isocurvature difficulties.

We realize the DAMP₀ scenario using supersymmetric models where the coupling between the Higgs and the inflaton results in a large axion mass during inflation. In particular, the inflaton energy density can induce a negative mass term for the Higgs, resulting in large Higgs VEVs in the D -flat direction. The quark masses that become larger due to the Higgs VEVs modify the RG running of the strong coupling constant and bring about a much larger QCD confinement scale. The axion mass is then enhanced by the high QCD scale, fulfilling the criteria for DAMP₀ in a consistent cosmology. We can also raise the QCD scale by means of generic moduli fields. The large Higgs field value is still crucial since otherwise the axion mass is suppressed by the small MSSM quark masses. In summary, the axion misalignment near the bottom of the potential can result from early dynamics and hence a small θ_{mis} can be regarded as a prediction of the model rather than fine-tuning.

BIBLIOGRAPHY

BIBLIOGRAPHY

- [1] Georges Aad et al. Observation of a new particle in the search for the Standard Model Higgs boson with the ATLAS detector at the LHC. *Phys. Lett. B*, 716:1–29, 2012.
- [2] L. F. Abbott and P. Sikivie. A Cosmological Bound on the Invisible Axion. *Phys. Lett.*, B120:133–136, 1983.
- [3] Bobby S. Acharya, Krzysztof Bozek, Miguel Crispim Romão, Stephen F. King, and Chakrit Pongkitivanichkul. Neutrino mass from M Theory SO(10). *JHEP*, 11:173, 2016.
- [4] Bobby S. Acharya, Sebastian A. R. Ellis, Gordon L. Kane, Brent D. Nelson, and Malcolm J. Perry. The lightest visible-sector supersymmetric particle is likely to be unstable. *Phys. Rev. Lett.*, 117:181802, 2016.
- [5] Bobby Samir Acharya. On Realizing N=1 superYang-Mills in M theory. 2000.
- [6] Bobby Samir Acharya and Konstantin Bobkov. Kahler Independence of the G(2)-MSSM. *JHEP*, 09:001, 2010.
- [7] Bobby Samir Acharya, Konstantin Bobkov, Gordon Kane, Piyush Kumar, and Diana Vaman. An M theory Solution to the Hierarchy Problem. *Phys. Rev. Lett.*, 97:191601, 2006.
- [8] Bobby Samir Acharya, Konstantin Bobkov, Gordon L. Kane, Piyush Kumar, and Jing Shao. Explaining the Electroweak Scale and Stabilizing Moduli in M Theory. *Phys. Rev. D*, 76:126010, 2007.
- [9] Bobby Samir Acharya, Konstantin Bobkov, Gordon L. Kane, Jing Shao, and Piyush Kumar. The G(2)-MSSM: An M Theory motivated model of Particle Physics. *Phys. Rev. D*, 78:065038, 2008.
- [10] Bobby Samir Acharya, Konstantin Bobkov, and Piyush Kumar. An M Theory Solution to the Strong CP Problem and Constraints on the Axiverse. *JHEP*, 11:105, 2010.
- [11] Bobby Samir Acharya and Sergei Gukov. M theory and singularities of exceptional holonomy manifolds. *Phys. Rept.*, 392:121–189, 2004.

- [12] Bobby Samir Acharya, Gordon Kane, and Eric Kuflik. Bounds on scalar masses in theories of moduli stabilization. *Int. J. Mod. Phys. A*, 29:1450073, 2014.
- [13] Bobby Samir Acharya, Gordon Kane, and Piyush Kumar. Compactified String Theories – Generic Predictions for Particle Physics. *Int. J. Mod. Phys. A*, 27:1230012, 2012.
- [14] Bobby Samir Acharya, Piyush Kumar, Konstantin Bobkov, Gordon Kane, Jing Shao, and Scott Watson. Non-thermal Dark Matter and the Moduli Problem in String Frameworks. *JHEP*, 06:064, 2008.
- [15] Bobby Samir Acharya and Edward Witten. Chiral fermions from manifolds of $G(2)$ holonomy. 2001.
- [16] P. A. R. Ade et al. Planck 2015 results. XIII. Cosmological parameters. *Astron. Astrophys.*, 594:A13, 2016.
- [17] Ian Affleck, Michael Dine, and Nathan Seiberg. Dynamical Supersymmetry Breaking in Supersymmetric QCD. *Nucl. Phys.*, B241:493–534, 1984.
- [18] Steven W. Allen, August E. Evrard, and Adam B. Mantz. Cosmological Parameters from Observations of Galaxy Clusters. *Ann. Rev. Astron. Astrophys.*, 49:409–470, 2011.
- [19] V. Anastassopoulos et al. Towards a medium-scale axion helioscope and haloscope. *JINST*, 12(11):P11019, 2017.
- [20] V. Andreev et al. Improved limit on the electric dipole moment of the electron. *Nature*, 562(7727):355–360, 2018.
- [21] E. Armengaud et al. Conceptual Design of the International Axion Observatory (IAXO). *JINST*, 9:T05002, 2014.
- [22] Asimina Arvanitaki, Savvas Dimopoulos, and Ken Van Tilburg. Resonant absorption of bosonic dark matter in molecules. *Phys. Rev.*, X8(4):041001, 2018.
- [23] Asimina Arvanitaki and Andrew A. Geraci. Resonantly Detecting Axion-Mediated Forces with Nuclear Magnetic Resonance. *Phys. Rev. Lett.*, 113(16):161801, 2014.
- [24] K. S. Babu, Borut Bajc, and Shaikh Saad. Yukawa Sector of Minimal $SO(10)$ Unification. *JHEP*, 02:136, 2017.
- [25] Kyu Jung Bae, Ji-Haeng Huh, and Jihn E. Kim. Update of axion CDM energy. *JCAP*, 0809:005, 2008.
- [26] C. A. Baker et al. An Improved experimental limit on the electric dipole moment of the neutron. *Phys. Rev. Lett.*, 97:131801, 2006.

- [27] Tom Banks and Michael Dine. The Cosmology of string theoretic axions. *Nucl. Phys.*, B505:445–460, 1997.
- [28] Stephen M. Barr. Solving the Strong CP Problem Without the Peccei-Quinn Symmetry. *Phys. Rev. Lett.*, 53:329, 1984.
- [29] Masha Baryakhtar, Junwu Huang, and Robert Lasenby. Axion and hidden photon dark matter detection with multilayer optical haloscopes. *Phys. Rev.*, D98(3):035006, 2018.
- [30] Chris Beasley, Jonathan J. Heckman, and Cumrun Vafa. GUTs and Exceptional Branes in F-theory - II: Experimental Predictions. *JHEP*, 01:059, 2009.
- [31] Luis Bento, Gustavo C. Branco, and Paulo A. Parada. A Minimal model with natural suppression of strong CP violation. *Phys. Lett.*, B267:95–99, 1991.
- [32] Dietrich Bodeker. Moduli decay in the hot early Universe. *JCAP*, 0606:027, 2006.
- [33] Claudio Bonati, Massimo D’Elia, Guido Martinelli, Francesco Negro, Francesco Sanfilippo, and Antonino Todaro. Topology in full QCD at high temperature: a multicanonical approach. *JHEP*, 11:170, 2018.
- [34] Sz. Borsanyi et al. Calculation of the axion mass based on high-temperature lattice quantum chromodynamics. *Nature*, 539(7627):69–71, 2016.
- [35] Jacob L. Bourjaily. Geometrically Engineering the Standard Model: Locally Unfolding Three Families out of E(8). *Phys. Rev.*, D76:046004, 2007.
- [36] Jacob L. Bourjaily. Local Models in F-Theory and M-Theory with Three Generations. 2009.
- [37] Andreas P. Braun, Sebastjan Cizel, Max Hübner, and Sakura Schäfer-Nameki. Higgs bundles for M-theory on G_2 -manifolds. *JHEP*, 03:199, 2019.
- [38] Matthew R. Buckley, David Feld, Sebastian Macaluso, Angelo Monteux, and David Shih. Cornering Natural SUSY at LHC Run II and Beyond. *JHEP*, 08:115, 2017.
- [39] Dmitry Budker, Peter W. Graham, Micah Ledbetter, Surjeet Rajendran, and Alex Sushkov. Proposal for a Cosmic Axion Spin Precession Experiment (CASPER). *Phys. Rev.*, X4(2):021030, 2014.
- [40] Florian Burger, Ernst-Michael Ilgenfritz, Maria Paola Lombardo, and Anton Trunin. Chiral observables and topology in hot QCD with two families of quarks. *Phys. Rev.*, D98(9):094501, 2018.
- [41] Nana Cabo Bizet, Albrecht Klemm, and Daniel Vieira Lopes. Landscaping with fluxes and the E8 Yukawa Point in F-theory. 2014.

- [42] Allen Caldwell, Gia Dvali, Béla Majorovits, Alexander Millar, Georg Raffelt, Javier Redondo, Olaf Reimann, Frank Simon, and Frank Steffen. Dielectric Haloscopes: A New Way to Detect Axion Dark Matter. *Phys. Rev. Lett.*, 118(9):091801, 2017.
- [43] J. A. Casas and C. Munoz. A Natural solution to the mu problem. *Phys. Lett.*, B306:288–294, 1993.
- [44] Cari Cesarotti, Qianshu Lu, Yuichiro Nakai, Aditya Parikh, and Matthew Reece. Interpreting the Electron EDM Constraint. 2018.
- [45] Kiwoon Choi, Eung Jin Chun, Sang Hui Im, and Kwang Sik Jeong. Diluting the inflationary axion fluctuation by a stronger QCD in the early Universe. *Phys. Lett.*, B750:26–30, 2015.
- [46] Kiwoon Choi, Hang Bae Kim, and Jihn E. Kim. Axion cosmology with a stronger QCD in the early universe. *Nucl. Phys.*, B490:349–364, 1997.
- [47] C. Herbert Clemens and Stuart Raby. Right-handed neutrinos and $U(1)_X$ symmetry-breaking. 2019.
- [48] Douglas Clowe, Marusa Bradac, Anthony H. Gonzalez, Maxim Markevitch, Scott W. Randall, Christine Jones, and Dennis Zaritsky. A direct empirical proof of the existence of dark matter. *Astrophys. J. Lett.*, 648:L109–L113, 2006.
- [49] Raymond T. Co, Eric Gonzalez, and Keisuke Harigaya. Axion Misalignment Driven to the Bottom. 2018.
- [50] Raymond T. Co, Eric Gonzalez, and Keisuke Harigaya. Axion Misalignment Driven to the Hilltop. 2018.
- [51] Raymond T. Co, Lawrence J. Hall, and Keisuke Harigaya. QCD Axion Dark Matter with a Small Decay Constant. *Phys. Rev. Lett.*, 120(21):211602, 2018.
- [52] Andrew G. Cohen, David B. Kaplan, and Ann E. Nelson. Counting 4 pis in strongly coupled supersymmetry. *Phys. Lett.*, B412:301–308, 1997.
- [53] R. J. Crewther, P. Di Vecchia, G. Veneziano, and Edward Witten. Chiral Estimate of the Electric Dipole Moment of the Neutron in Quantum Chromodynamics. *Phys. Lett.*, 88B:123, 1979. [Erratum: *Phys. Lett.* 91B,487(1980)].
- [54] Richard Lynn Davis. Cosmic Axions from Cosmic Strings. *Phys. Lett.*, B180:225–230, 1986.
- [55] S. Dimopoulos and L. J. Hall. Inflation and Invisible Axions. *Phys. Rev. Lett.*, 60:1899–1901, 1988.
- [56] Michael Dine and Willy Fischler. The Not So Harmless Axion. *Phys. Lett.*, B120:137–141, 1983.

- [57] Michael Dine, Willy Fischler, and Mark Srednicki. A Simple Solution to the Strong CP Problem with a Harmless Axion. *Phys. Lett. B*, 104:199–202, 1981.
- [58] N. Du et al. A Search for Invisible Axion Dark Matter with the Axion Dark Matter Experiment. *Phys. Rev. Lett.*, 120(15):151301, 2018.
- [59] Emilian Dudas and Eran Palti. Froggatt-Nielsen models from E(8) in F-theory GUTs. *JHEP*, 01:127, 2010.
- [60] G. R. Dvali. Removing the cosmological bound on the axion scale. 1995.
- [61] John R. Ellis and Mary K. Gaillard. Strong and Weak CP Violation. *Nucl. Phys.*, B150:141–162, 1979.
- [62] John R. Ellis and Keith A. Olive. Constraints on Light Particles From Supernova Sn1987a. *Phys. Lett.*, B193:525, 1987.
- [63] Sebastian A. R. Ellis, Gordon L. Kane, and Bob Zheng. Superpartners at LHC and Future Colliders: Predictions from Constrained Compactified M-Theory. *JHEP*, 07:081, 2015.
- [64] Jarah Evslin. From E(8) to F via T. *JHEP*, 08:021, 2004.
- [65] S. M. Faber and R. E. Jackson. Velocity dispersions and mass to light ratios for elliptical galaxies. *Astrophys. J.*, 204:668, 1976.
- [66] Daniel Feldman, Zuowei Liu, and Pran Nath. The Stueckelberg Z-prime Extension with Kinetic Mixing and Milli-Charged Dark Matter From the Hidden Sector. *Phys. Rev. D*, 75:115001, 2007.
- [67] D. J. Fixsen. The Temperature of the Cosmic Microwave Background. *The Astrophysical Journal*, 707(2):916–920, 2009.
- [68] Davide Gaiotto, Gregory W. Moore, and Edward Witten. Algebra of the Infrared: String Field Theoretic Structures in Massive $\mathcal{N} = (2, 2)$ Field Theory In Two Dimensions. 2015.
- [69] Howard Georgi and Lisa Randall. Flavor Conserving CP Violation in Invisible Axion Models. *Nucl. Phys.*, B276:241–252, 1986.
- [70] A. A. Geraci et al. Progress on the ARIADNE axion experiment. *Springer Proc. Phys.*, 211:151–161, 2018.
- [71] Hadi Godazgar, Mahdi Godazgar, and Malcolm J. Perry. E8 duality and dual gravity. *JHEP*, 06:044, 2013.
- [72] Mark W. Goodman and Edward Witten. Global Symmetries in Four-dimensions and Higher Dimensions. *Nucl. Phys.*, B271:21–52, 1986.

- [73] Marco Gorghetto and Giovanni Villadoro. Topological Susceptibility and QCD Axion Mass: QED and NNLO corrections. 2018.
- [74] Peter W. Graham and Adam Scherlis. Stochastic axion scenario. *Phys. Rev.*, D98(3):035017, 2018.
- [75] Michael B. Green and John H. Schwarz. Anomaly Cancellation in Supersymmetric D=10 Gauge Theory and Superstring Theory. *Phys. Lett. B*, 149:117–122, 1984.
- [76] Patrick B. Greene, Lev Kofman, and Alexei A. Starobinsky. Sine-Gordon parametric resonance. *Nucl. Phys.*, B543:423–443, 1999.
- [77] Alan H. Guth. The Inflationary Universe: A Possible Solution to the Horizon and Flatness Problems. *Phys. Rev. D*, 23:347–356, 1981.
- [78] Lawrence J. Hall and Stuart Raby. A Complete supersymmetric SO(10) model. *Phys. Rev.*, D51:6524–6531, 1995.
- [79] Keisuke Harigaya, Masahiro Ibe, Kai Schmitz, and Tsutomu T. Yanagida. Peccei-Quinn Symmetry from Dynamical Supersymmetry Breaking. *Phys. Rev.*, D92(7):075003, 2015.
- [80] Keisuke Harigaya, Masahiro Ibe, and Motoo Suzuki. Mass-splitting between haves and have-nots - symmetry vs. Grand Unified Theory. *JHEP*, 09:155, 2015.
- [81] Keisuke Harigaya and Masahiro Kawasaki. QCD axion dark matter from long-lived domain walls during matter domination. *Phys. Lett.*, B782:1–5, 2018.
- [82] Keisuke Harigaya and Jacob Leedom. Unified Models of the QCD Axion and Supersymmetry Breaking. *Nucl. Phys.*, B921:507–521, 2017.
- [83] Keisuke Harigaya and Kyohei Mukaida. Thermalization after/during Reheating. *JHEP*, 05:006, 2014.
- [84] Tetsutaro Higaki, Kwang Sik Jeong, and Fuminobu Takahashi. Solving the Tension between High-Scale Inflation and Axion Isocurvature Perturbations. *Phys. Lett.*, B734:21–26, 2014.
- [85] Gudrun Hiller and Martin Schmaltz. Solving the Strong CP Problem with Supersymmetry. *Phys. Lett.*, B514:263–268, 2001.
- [86] G. Hinshaw et al. Nine-Year Wilkinson Microwave Anisotropy Probe (WMAP) Observations: Cosmological Parameter Results. *Astrophys. J. Suppl.*, 208:19, 2013.
- [87] Takashi Hiramatsu, Masahiro Kawasaki, and Ken’ichi Saikawa. Evolution of String-Wall Networks and Axionic Domain Wall Problem. *JCAP*, 1108:030, 2011.

- [88] Takashi Hiramatsu, Masahiro Kawasaki, Ken'ichi Saikawa, and Toyokazu Sekiguchi. Axion cosmology with long-lived domain walls. *JCAP*, 1301:001, 2013.
- [89] Seyda Ipek and Tim M. P. Tait. An Early Cosmological Period of QCD Confinement. 2018.
- [90] R. Jackiw and C. Rebbi. Vacuum Periodicity in a Yang-Mills Quantum Theory. *Phys. Rev. Lett.*, 37:172–175, 1976.
- [91] Kwang Sik Jeong and Fuminobu Takahashi. Suppressing Isocurvature Perturbations of QCD Axion Dark Matter. *Phys. Lett.*, B727:448–451, 2013.
- [92] Yonatan Kahn, Benjamin R. Safdi, and Jesse Thaler. Broadband and Resonant Approaches to Axion Dark Matter Detection. *Phys. Rev. Lett.*, 117(14):141801, 2016.
- [93] Gordon Kane, Piyush Kumar, and Jing Shao. CP-violating Phases in M-theory and Implications for EDMs. *Phys. Rev. D*, 82:055005, 2010.
- [94] Gordon Kane and Martin Wolfgang Winkler. Deriving the Inflaton in Compactified M-theory with a De Sitter Vacuum. *Phys. Rev.*, D100(6):066005, 2019.
- [95] Gordon Kane and Martin Wolfgang Winkler. Baryogenesis from a Modulus Dominated Universe. *JCAP*, 2002(02):019, 2020.
- [96] Sheldon Katz and David R. Morrison. Gorenstein Threefold Singularities with Small Resolutions via Invariant Theory for Weyl Groups. *J. Alg. Geom.*, 1(3):449–530, 1992.
- [97] Sheldon H. Katz and Cumrun Vafa. Matter from Geometry. *Nucl. Phys.*, B497:146–154, 1997.
- [98] Masahiro Kawasaki, Ken'ichi Saikawa, and Toyokazu Sekiguchi. Axion dark matter from topological defects. *Phys. Rev.*, D91(6):065014, 2015.
- [99] Masahiro Kawasaki, Fuminobu Takahashi, and Masaki Yamada. Suppressing the QCD Axion Abundance by Hidden Monopoles. *Phys. Lett.*, B753:677–681, 2016.
- [100] Masahiro Kawasaki, Masaki Yamada, and Tsutomu T. Yanagida. Cosmologically safe QCD axion as a present from extra dimension. *Phys. Lett.*, B750:12–16, 2015.
- [101] John Kearney, Nicholas Orlofsky, and Aaron Pierce. High-Scale Axions without Isocurvature from Inflationary Dynamics. *Phys. Rev.*, D93(9):095026, 2016.

- [102] I. B. Khriplovich and A. R. Zhitnitsky. What Is the Value of the Neutron Electric Dipole Moment in the Kobayashi-Maskawa Model? *Phys. Lett.*, 109B:490–492, 1982.
- [103] Jihn E. Kim. Weak Interaction Singlet and Strong CP Invariance. *Phys. Rev. Lett.*, 43:103, 1979.
- [104] Vincent B. Klaer and Guy D. Moore. The dark-matter axion mass. *JCAP*, 1711(11):049, 2017.
- [105] Edward W. Kolb and Igor I. Tkachev. Axion miniclusters and Bose stars. *Phys. Rev. Lett.*, 71:3051–3054, 1993.
- [106] Edward W. Kolb and Igor I. Tkachev. Nonlinear axion dynamics and formation of cosmological pseudosolitons. *Phys. Rev.*, D49:5040–5051, 1994.
- [107] Edward W. Kolb and Michael S. Turner. *The Early Universe*, volume 69. 1990.
- [108] Markus A. Luty. Naive dimensional analysis and supersymmetry. *Phys. Rev.*, D57:1531–1538, 1998.
- [109] D. H. Lyth. Axions and inflation: Sitting in the vacuum. *Phys. Rev.*, D45:3394–3404, 1992.
- [110] Aneesh Manohar and Howard Georgi. Chiral Quarks and the Nonrelativistic Quark Model. *Nucl. Phys.*, B234:189–212, 1984.
- [111] Fernando Marchesano, Diego Regalado, and Gianluca Zoccarato. Yukawa hierarchies at the point of E_8 in F-theory. *JHEP*, 04:179, 2015.
- [112] Stephen P. Martin. A Supersymmetry primer. *Adv. Ser. Direct. High Energy Phys.*, 18:1–98, 1998.
- [113] Ron Mayle, James R. Wilson, John R. Ellis, Keith A. Olive, David N. Schramm, and Gary Steigman. Constraints on Axions from SN 1987a. *Phys. Lett.*, B203:188–196, 1988.
- [114] Kyohei Mukaida and Kazunori Nakayama. Dynamics of oscillating scalar field in thermal environment. *JCAP*, 1301:017, 2013.
- [115] Priyamvada Natarajan et al. Mapping substructure in the HST Frontier Fields cluster lenses and in cosmological simulations. *Mon. Not. Roy. Astron. Soc.*, 468(2):1962–1980, 2017.
- [116] Ann E. Nelson. Naturally Weak CP Violation. *Phys. Lett.*, 136B:387–391, 1984.
- [117] Hans Peter Nilles and Stuart Raby. Supersymmetry and the strong CP problem. *Nucl. Phys.*, B198:102–112, 1982.

- [118] Yasunori Nomura, Surjeet Rajendran, and Fabio Sanches. Axion Isocurvature and Magnetic Monopoles. *Phys. Rev. Lett.*, 116(14):141803, 2016.
- [119] Hiroshi Ooguri and Cumrun Vafa. On the Geometry of the String Landscape and the Swampland. *Nucl. Phys. B*, 766:21–33, 2007.
- [120] Jonathan L. Ouellet et al. First Results from ABRACADABRA-10 cm: A Search for Sub- μeV Axion Dark Matter. *Phys. Rev. Lett.*, 122(12):121802, 2019.
- [121] Eran Palti. Wavefunctions and the Point of E_8 in F-theory. *JHEP*, 07:065, 2012.
- [122] Tony Pantev and Martijn Wijnholt. Hitchin’s Equations and M-Theory Phenomenology. *J. Geom. Phys.*, 61:1223–1247, 2011.
- [123] R. D. Peccei and Helen R. Quinn. Constraints Imposed by CP Conservation in the Presence of Instantons. *Phys. Rev.*, D16:1791–1797, 1977.
- [124] R. D. Peccei and Helen R. Quinn. CP Conservation in the Presence of Instantons. *Phys. Rev. Lett.*, 38:1440–1443, 1977.
- [125] Peter Petreczky, Hans-Peter Schadler, and Sayantan Sharma. The topological susceptibility in finite temperature QCD and axion cosmology. *Phys. Lett.*, B762:498–505, 2016.
- [126] Maxim Pospelov and Adam Ritz. Theta vacua, QCD sum rules, and the neutron electric dipole moment. *Nucl. Phys. B*, 573:177–200, 2000.
- [127] John Preskill, Mark B. Wise, and Frank Wilczek. Cosmology of the Invisible Axion. *Phys. Lett.*, B120:127–132, 1983.
- [128] Georg Raffelt and David Seckel. Bounds on Exotic Particle Interactions from SN 1987a. *Phys. Rev. Lett.*, 60:1793, 1988.
- [129] Georg G. Raffelt. Astrophysical axion bounds. *Lect. Notes Phys.*, 741:51–71, 2008.
- [130] Alexandre Refregier. Weak gravitational lensing by large scale structure. *Ann. Rev. Astron. Astrophys.*, 41:645–668, 2003.
- [131] Graham Ross and Mario Serna. Unification and fermion mass structure. *Phys. Lett. B*, 664:97–102, 2008.
- [132] Vera C. Rubin and W. Kent Ford, Jr. Rotation of the Andromeda Nebula from a Spectroscopic Survey of Emission Regions. *Astrophys. J.*, 159:379–403, 1970.
- [133] Gray Rybka, Andrew Wagner, Aryeh Brill, Katleiah Ramos, Robert Percival, and Kunal Patel. Search for dark matter axions with the Orpheus experiment. *Phys. Rev.*, D91(1):011701, 2015.

- [134] Joel Scherk and John H. Schwarz. Dual Models for Nonhadrons. *Nucl. Phys. B*, 81:118–144, 1974.
- [135] Mikhail A. Shifman, A. I. Vainshtein, and Valentin I. Zakharov. Can Confinement Ensure Natural CP Invariance of Strong Interactions? *Nucl. Phys.*, B166:493–506, 1980.
- [136] P. Sikivie. Axion Dark Matter Detection using Atomic Transitions. *Phys. Rev. Lett.*, 113(20):201301, 2014.
- [137] Karl Strobl and Thomas J. Weiler. Anharmonic evolution of the cosmic axion density spectrum. *Phys. Rev.*, D50:7690–7702, 1994.
- [138] Peter Svrcek and Edward Witten. Axions In String Theory. *JHEP*, 06:051, 2006.
- [139] Gerard 't Hooft. Symmetry Breaking Through Bell-Jackiw Anomalies. *Phys. Rev. Lett.*, 37:8–11, 1976.
- [140] Gerard 't Hooft and M. J. G. Veltman. One loop divergencies in the theory of gravitation. *Ann. Inst. H. Poincare Phys. Theor. A*, 20:69–94, 1974.
- [141] Fuminobu Takahashi and Masaki Yamada. Strongly broken Peccei-Quinn symmetry in the early Universe. *JCAP*, 1510(10):010, 2015.
- [142] Fuminobu Takahashi, Wen Yin, and Alan H. Guth. QCD axion window and low-scale inflation. *Phys. Rev.*, D98(1):015042, 2018.
- [143] M. Tanabashi et al. Review of Particle Physics. *Phys. Rev. D*, 98(3):030001, 2018.
- [144] Michael S. Turner. Cosmic and Local Mass Density of Invisible Axions. *Phys. Rev.*, D33:889–896, 1986.
- [145] Michael S. Turner. Axions from SN 1987a. *Phys. Rev. Lett.*, 60:1797, 1988.
- [146] G. Veneziano. Construction of a crossing - symmetric, Regge behaved amplitude for linearly rising trajectories. *Nuovo Cim. A*, 57:190–197, 1968.
- [147] Luca Visinelli and Paolo Gondolo. Dark Matter Axions Revisited. *Phys. Rev.*, D80:035024, 2009.
- [148] J. K. Vogel et al. IAXO - The International Axion Observatory. In *8th Patras Workshop on Axions, WIMPs and WISPs (AXION-WIMP 2012) Chicago, Illinois, July 18-22, 2012*, 2013.
- [149] Steven Weinberg. A New Light Boson? *Phys. Rev. Lett.*, 40:223–226, 1978.
- [150] Frank Wilczek. Problem of Strong P and T Invariance in the Presence of Instantons. *Phys. Rev. Lett.*, 40:279–282, 1978.

- [151] Mark B. Wise, Howard Georgi, and Sheldon L. Glashow. SU(5) and the Invisible Axion. *Phys. Rev. Lett.*, 47:402, 1981.
- [152] Edward Witten. String theory dynamics in various dimensions. *Nucl. Phys. B*, 443:85–126, 1995.
- [153] Edward Witten. Deconstruction, G(2) holonomy, and doublet triplet splitting. In *Supersymmetry and unification of fundamental interactions. Proceedings, 10th International Conference, SUSY'02, Hamburg, Germany, June 17-23, 2002*, pages 472–491, 2001.
- [154] A. R. Zhitnitsky. On Possible Suppression of the Axion Hadron Interactions. (In Russian). *Sov. J. Nucl. Phys.*, 31:260, 1980. [*Yad. Fiz.*31,497(1980)].
- [155] F. Zwicky. Die Rotverschiebung von extragalaktischen Nebeln. *Helv. Phys. Acta*, 6:110–127, 1933.
- [156] F. Zwicky. On the Masses of Nebulae and of Clusters of Nebulae. *Astrophys. J.*, 86:217–246, 1937.
- [157] P. A. Zyla et al. Review of Particle Physics. *PTEP*, 2020(8):083C01, 2020.